

**Some Problems in the Mathematics of Fracture:
Paths From Front Kinetics and a Level Set Method**

by

Casey Lyndale Richardson

A Dissertation

Submitted to the Faculty

of

WORCESTER POLYTECHNIC INSTITUTE

In partial fulfillment of the requirements for the

Degree of Doctor of Philosophy

in

Mathematical Sciences

by

April 21, 2008

APPROVED:

Professor Christopher J. Larsen
Dissertation Advisor
Department of Mathematical Sciences
Worcester Polytechnic Institute

Professor Gilles Francfort
Département de Mathématiques
Université Paris-Nord

Professor Konstantin Lurie
Department of Mathematical Sciences
Worcester Polytechnic Institute

Professor Michael Ortiz
Division of Engineering and Applied Science
California Institute of Technology

Professor Marcus Sarkis
Department of Mathematical Sciences
Worcester Polytechnic Institute

To Marsha, my wife and best friend, with love.

Acknowledgments

My time as a Ph.D. student has certainly been challenging, both professionally and personally, but it has been an extremely rewarding five years. I truly feel privileged to have had these experiences, and I am deeply thankful to everyone who has made them possible and helped me during my graduate program.

So much of the value of these years has come from working with my advisor, Chris Larsen. I thank him for introducing me to such interesting and challenging problems, and providing guidance, problem-solving advice, and mathematical insight in the pursuit of understanding those problems.

I am very grateful to have collaborated with Michael Ortiz, Marcus Sarkis, and Blaise Bourdin. They have taught me so much and working with them has led to fantastic experiences and opportunities, in many parts of the world. While working on my research, I have also greatly benefitted from many conversations with Gilles Francfort. I would also like to thank Christoph Ortner, who provided many helpful corrections and improvements on an earlier draft of the work presented in Chapter 2.

I extend my sincere appreciation to the members of my dissertation committee: Professor Larsen, Professor Ortiz, Professor Francfort, Professor Konstantin Lurie, and Professor Sarkis, and to my professional references: Professor Larsen, Professor Francfort, Professor Ortiz and Professor William Farr.

I would like to thank the faculty, staff, and students of the WPI Mathematical Sciences Department for their help and support during my time in the Ph.D. program. In particular, I appreciate the support and friendship of my fellow graduate students, and the help of Linda Bullens, Ellen Mackin, Debbie Riel and Mike Malone.

Over the course of my graduate program, I have benefitted tremendously from several grants, which have supported my research assistantship and provided funds for me to travel to conferences and summer schools. These include a grant from the NSF to my advisor, an NSF grant to Professor Sarkis, a travel award to Brazil through the Consortium of the Americas for Interdisciplinary Science recommended by Professor Sarkis, and travel funds from the NSF Oberwolfach Junior Fellowship program.

I conclude these acknowledgements by thanking my family for their constant support. First and foremost, I thank my wife, Marsha, for her patience, support, and love over these last five years. Together, we have worked hard and sacrificed many things to achieve this goal, and I dedicate this work to her. I thank my Mom and Dad for all that they have done for me; if I have or will accomplish anything, it is because of their hard work and love. Last, but certainly not least, I sincerely appreciate the support of my siblings Heidi, Travis, Mike, Julie, Maggie, John, Shane, and Jeff, as well as my extended family Norm & Sheila, Ray & Sherri, and Mandy.

Contents

1	Introduction	1
1.1	Background	1
1.2	Overview of Dissertation	3
2	Fracture Paths From Front Kinetics	5
2.1	Introduction	5
2.2	Minimum principles for rate problems in mechanics	8
2.3	Fracture mechanics as a rate problem	10
2.4	Notation and mathematical setting	18
2.5	Existence for constrained trajectories	20
2.6	Relaxation and Rate-Independence	28
2.6.1	Definitions	29
2.6.2	Convergence of Trajectories	30
2.6.3	Relaxation Theorem	35
3	A Level Set Method for Mumford-Shah and Fracture	61
3.1	Introduction	61
3.2	Revisiting the Vese-Chan algorithm	64
3.2.1	Crack-tips	64
3.2.2	Triple junctions	65
3.2.3	The Four Color Theorem	66
3.3	Introduction to the proposed level set algorithm	67
3.4	The new level set method	69
3.4.1	Formal Description	69
3.4.2	Computational details	70
3.5	Numerical results	74
	Table of Notation	77

Chapter 1

Introduction

This dissertation is focused on certain variational models of fracture. In engineering, the design of structures that can resist cracking is an important goal, with implications for structural performance and safety. The development of well-posed models of fracture that can predict the paths of cracks is both a critical step to achieving this goal and a challenging mathematical problem. Also, the analytical results are all quite recent because the mathematical tools necessary for formulating a variational fracture model were developed within the last twenty years. These recent developments have generated interest in rigorous analysis of fracture models, built upon collaboration between the math and engineering communities.

In this chapter, I will set the stage for the results presented in this dissertation. First, in Section 1.1, I will provide some background on variational models of fracture; my goals for that section are to provide some historical context, introduce some of the notation, and to survey useful references. Then, in Section 1.2, I will give a brief description of the results presented in this dissertation.

1.1 Background

In the context of modelling fracture, the primary goal is to formulate a well-posed model that can *predict crack evolution*, which includes determining both when pre-existing cracks will run and the paths that such cracks take through the material. Although models with such predictive capability are quite recent, the central idea in the theory of brittle fracture was proposed by Griffith in 1920 [18]. He formulated the following criterion for two dimensional crack propagation: a pre-existing crack can run only when the

elastic energy that is released by cracking, per unit length of crack, exceeds the toughness of the material. Precisely, he defined the energy release rate (in two dimensions) as:

$$G := -\frac{dE}{dl}$$

where E is the bulk elastic energy stored in the material and l is the length of the crack. Then, the *Griffith criterion* states that the crack will not run if G is less than the toughness of the material, and can run if G equals the toughness. Implicit in this criterion is a view of fracture as a balance between the energy that is required to create new crack - which Griffith implied is proportional to the length of the crack - and the elastic energy that is released when the material cracks. However, notice that the Griffith criterion only provides a rule for determining when cracks grow; the path of the crack must be known *a priori* (see Figure 1.1).

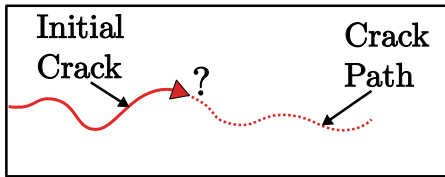


Figure 1.1: Typical setting for Griffith criterion.

This assumption and the restriction to two dimensions were eliminated using methods in the Calculus of Variations. The main ingredient was the appropriate space of candidate functions, the so called Special Functions of Bounded Variation (SBV), first analyzed by Ambrosio and De Giorgi [14]. Briefly stated, $SBV(\Omega)$ is the space of functions $u \in BV(\Omega)$ such that the singular part of Du is concentrated on the set where u is (approximately) discontinuous, a set of codimension 1 (see [15] [4] [30] for a complete description). Using $u \in SBV(\Omega)$ to map Ω to its deformed configuration, with the discontinuity set of u identifying the crack set, Ambrosio and Braides [3] proposed to model static fracture by minimizing

$$u \mapsto \int_{\Omega} W(\nabla u) dx + \mathcal{H}^{N-1}(S(u)) \quad (1.1.1)$$

over $u \in SBV(\Omega)$, $u = g$ (given) on $\partial\Omega$; here W is the elastic energy density, $S(u)$ denotes the set of (approximate) discontinuity points of u , and $\nabla u dx$ is the absolutely

continuous part of Du . Notice that for an admissible function, one can generally create a competitor with lower elastic energy by using more discontinuities, but at the cost of the “length” of the additional discontinuity set. Thus (1.1.1) captures the competition between crack length and elastic energy release that is the core feature of the Griffith criterion, and the location of the crack is determined by this energy minimization. The existence of a minimizer for (1.1.1), given typical assumptions on W , follows from the compactness of the space SBV , first proved by Ambrosio [2].

For crack evolution, the only analytical results are for *quasistatic* evolutions, meaning that the rate of change in the problem parameters (Dirichlet boundary conditions, boundary loads, body forces) is small compared to the time it takes the body to reach elastic equilibrium. Francfort and Marigo [17] proposed the following model: first discretize time, at each timestep solve an appropriate static problem (where, since cracks cannot heal, (1.1.1) is slightly modified to penalize only new discontinuities), and then find the time continuous evolution by taking the limit as the size of the timesteps goes to zero. The main issue is to show that this limit satisfies the properties of a quasistatic evolution: loosely stated, at each time the crack set and deformation satisfy a minimality property and that the crack evolution satisfies an energy balance, which relates the stored elastic energy plus the dissipated energy to the work done by loading. These properties were proved for the time continuous limit, first in two dimensions with certain geometric constraints on the crack sets by Dal Maso and Toader [11], and then in the general setting by Francfort and Larsen [16] and Dal Maso, Francfort and Toader [12].

1.2 Overview of Dissertation

The results presented in this dissertation involve two separate problems, with the remaining two chapters divided accordingly. Chapter 2 presents the first problem; this chapter reproduces the presentation in [19], with only slight modifications and some additional figures. The work involved developing and analyzing models of fracture in which we modeled the energy dissipated by crack growth as concentrated on the front of the crack, a set of codimension 2. It is natural to suppose that, as the crack propagates, the dissipated energy should be local to where the crack is growing and depend on the local speed of crack growth. While many engineering models of fracture are based on some notion of crack front, there had not been a rigorous definition of front, let alone mathematical analysis of a front-based fracture model. We presented the first work in

this direction including:

- The first rigorous definition of crack front and front speed (See (2.1.1))
- A model of fracture whose evolution law is described at the crack front using the front speed (See (2.1.2))
- A new (and equivalent) way of enforcing the irreversibility of fracture (Remark 2.6.3)
- An existence result for a constrained version of this front-based model (Theorem 2.5.2)
- A relaxation result (Theorem 2.6.13) that:
 - Holds in any dimension
 - Completely characterizes the optimal front microstructure
 - Shows the surprising result that the effective energy is always rate-independent
- A proof that any crack evolution can be approximated strongly from within by an evolution with a front moving arbitrarily close to any desired speed (Theorem 2.6.12).

Chapter 3 contains a level set method for computing stationary points for the Mumford-Shah functional (from image segmentation) and fracture; as above, the chapter follows the presentation in [20]. Generally, the idea behind level set methods is to associate the singular set with the zero level set of some function. This function evolves, governed by a PDE that is similar to that of motion by mean curvature, so that the zero level set moves to a stationary point of the functional. In [20], we proposed a new technique that addresses several issues unresolved by previous techniques. Our method:

- Can handle tips in the singular sets (important for fracture)
- Can find minimizers that previous techniques cannot find, in particular when the minimizing singular set contains triple junctions (see Section 3.5).

The implementation of this technique involved a Matlab finite element code (adapted from [1]) for computing solutions to the associated elliptic PDE and the use of mesh generation tools [27]. Some of the numerical challenges were stability, for which we used a Lax-Freidrichs descretization with local timestepping, and the choice of appropriate interpolation algorithms to compute curvatures.

Chapter 2

Fracture Paths From Front Kinetics

2.1 Introduction

The goal of the work presented in this chapter is to model the energy dissipation due to cracking as concentrated on crack fronts, and therefore generalize the Griffith dissipation used in (1.1.1). This goal is motivated by the following observation: when a material fractures, the energy that is dissipated by cracking should be local to where the crack is growing, and should depend on the local speed of crack growth. Most engineering models of fracture are formulated using some notion of a crack tip or front, and front speed, but such ideas had not been investigated rigorously. A critical first step of this work was to rigorously define these two notions.

Then, given such definitions, one can view penalizing the length of the crack (as in (1.1.1)) as a dissipation that depends linearly on the front speed. A precise definition of crack front and front speed then allows the use of dissipations with a *nonlinear dependence* on the front speed. Therefore, our next step was to pose a variational model with such a dissipation, and understand the resulting optimal microstructure with the aim of proving existence of minimizers. In this chapter, which closely follows the presentation in [19], I present our results for these questions, some of which were quite surprising.

First, I now introduce our definition of crack front, which is formulated using the entire trajectory of crack evolution. Specifically, we consider the class of trajectories u with corresponding *crack trajectory* C that is increasing and such that at each time t the discontinuity set $S(u(t))$ is a subset of $C(t)$ (up to a set of \mathcal{H}^{N-1} measure zero). Furthermore, the crack trajectory has a *front representation*, i.e., there exists a function

$F : [0, T] \rightarrow 2^\Omega$, and a family of functions $v(\cdot, t) : F(t) \rightarrow \mathbb{R}$, such that

$$\int_0^T \dot{\varphi}(t) \int_{C(t)} f(x) d\mathcal{H}^{N-1}(x) dt = - \int_0^T \varphi(t) \int_{F(t)} f(x) v(x, t) d\mathcal{H}^{N-2}(x) dt \quad (2.1.1)$$

$$\forall \varphi \in C_0^1([0, T]), \forall f \in C_0(\Omega')$$

where $\Omega \subset\subset \Omega'$. We call the set $F(t)$ the *crack front* or *front* at time t , and v the *front speed*. Note that if (u, C) satisfies (2.1.1) then necessarily the measure of C is absolutely continuous in time; however, it is unclear if absolute continuity is sufficient. A quick calculation also shows that restricting to trajectories with $v \geq 0$ provides a new and equivalent way of enforcing the irreversibility of fracture, i.e., the monotonicity of C .

With this class we formulated our model. We could have used the incremental minimization approach described in Section 1.1 (see Remark 2.3.1), but it is somewhat more natural to use the new energy functionals of Mielke-Ortiz (see [22]), which are functionals designed to model dissipative systems using *entire trajectories of the system*. Thus, our model is the following: for given $\psi : [0, \infty) \rightarrow [0, \infty)$, find (u_ϵ, C_ϵ) by minimizing

$$I_\epsilon[u] := \int_0^T e^{-\frac{t}{\epsilon}} \left\{ \frac{1}{\epsilon} \int_\Omega W(\nabla u(x, t)) dx + \int_{F(t)} \psi(v(x, t)) d\mathcal{H}^{N-2}(x) \right\} dt, \quad (2.1.2)$$

over the class of front representable trajectories (matching given boundary conditions), and then take the limit as $\epsilon \rightarrow 0$ to recover the quasistatic evolution.

A critical fact about this class of trajectories is that in order for a minimizing sequence $\{u_i\}_{i=1}^\infty$ of (2.1.2) to converge (in the natural sense, to be described later) to a trajectory u with corresponding crack C having a front representation, it is necessary that ψ have superlinear growth at infinity, but this is *not sufficient*. There are two reasons for this lack of compactness. First, it is possible that the discontinuity sets of the u_i close up as $i \rightarrow \infty$ only for t within some time interval, so that the limit u has discontinuity sets that appear instantaneously at the end of this interval. Second, these sequences can have crack sets that exhibit the onset of a *mother-daughter* microstructure, meaning that the crack grows by creating many small cracks just ahead of the macroscopic crack front, effectively bypassing the superlinear growth of ψ .

Our approach to the first issue is a weakening of the natural choice of C for a given trajectory u – that $C(t)$ is the smallest crack set containing all prior discontinuities of u . Instead, we only require the inclusion of discontinuity sets, namely, that up to sets

of \mathcal{H}^{N-1} measure zero,

$$S(u(\tau)) \subset C(t) \quad \forall \tau \in [0, t].$$

We will present two approaches to the second issue, organized in this chapter as follows. In Section 2.5 we will constrain the admissible trajectories to prevent mother-daughter type microstructures and ensure compactness of our constrained class. The corresponding variational problem is analyzed in a two dimensional setting, finally showing the existence of an optimal crack path (Theorem 2.5.2).

Section 2.6 presents the central result of our work. In that section, we allow such microstructures generally, in N dimensions and without constraints on admissible trajectories, which requires relaxation. We show that the mother-daughter mechanism is only part of the picture, and in fact minimizing sequences will employ a front microstructure that enables them to move at an energetically optimal front speed, which *depends only on the linear envelope of the function ψ* . We thereby show that, remarkably, any energy whose dissipation rate is of the form

$$\int_{F(t)} \psi(v) d\mathcal{H}^{N-2}$$

relaxes to an energy whose dissipation rate is proportional to the front speed, i. e., a rate-independent dissipation, and so also a Griffith energy dissipation (Theorem 2.6.13).

Perhaps the most natural example for which we would not have expected relaxation to a rate-independent dissipation is $\psi(v) = \alpha + v^p$, giving the energy

$$I_\epsilon[u, C] = \int_0^T e^{-\frac{t}{\epsilon}} \left\{ \frac{1}{\epsilon} \int_{\Omega} W(\nabla u(x, t)) dx + \int_{F(t)} (\alpha + v^p(x, t)) d\mathcal{H}^{N-2}(x) \right\} dt, \quad (2.1.3)$$

with $\alpha > 0$ and $p > 1$. While it would seem that having a fixed penalty on the front size and a superlinear penalty on the front speed would prevent microstructure, let alone relaxation to rate-independence, the relaxation result of Theorem 2.6.13 shows that this is not the case.

2.2 Minimum principles for rate problems in mechanics

Many physical systems are governed by problems of the *rate form*. Thus, let $u \in Y$ be a field that describes the state of the system, where Y is the corresponding configuration space. For the systems under consideration, the trajectory $u : (0, T) \rightarrow Y$ over a time interval $(0, T)$ is governed by the problem:

$$u(0) = u_0 \quad (2.2.4a)$$

$$\dot{u}(t) = v(t) \quad (2.2.4b)$$

$$v(t) \in \operatorname{argmin}\{G(t, u(t), v(t))\} \quad (2.2.4c)$$

where $\dot{u}(t)$ is the time derivative, or *rate*, of u at time t ; $u_0 \in Y$ is the initial state of the system; and $G : (0, T) \times Y \times Y \rightarrow \bar{\mathbb{R}}$ is a rate functional. Problem (2.2.4) entails a sequence of minimum problems parameterized by time. For every time, the minimum problem (2.2.4c), or *rate problem*, returns the rate $v(t)$ corresponding to the known state $u(t)$. Integration of these rates in time then determines the evolution of the system.

A special example of rate problem (2.2.4c) arises in evolutionary problems governed by rate equations of the form

$$0 \in \partial\Psi(\dot{u}(t)) + DE(t, u(t)), \quad (2.2.5a)$$

$$u(0) = u_0, \quad (2.2.5b)$$

where $\Psi : Y \rightarrow \mathbb{R}_\infty := \mathbb{R} \cup \{\infty\}$ is a convex dissipation potential; $E : Y \rightarrow \mathbb{R}_\infty$ is an energy function; $\partial\Psi$ is the subdifferential of Ψ , representing the system of dissipative forces; DE is the Fréchet derivative of E , representing the conservative force system; and time t varies in the interval $[0, T]$. Equation (2.2.5a) establishes a balance between dissipative forces and conservative forces, and the trajectory $u(t)$ of the system is the result of this balance and of the initial condition (2.2.5b). In this particular case, the rate functional takes the *additive* form

$$G(t, u(t), v(t)) = \Psi(v(t)) + DE(t, u(t))v(t). \quad (2.2.6)$$

Whereas, for fixed time, the rate of evolution of the system is characterized vari-

ationally by the rate problem (2.2.4c), the trajectories of the system lack an obvious variational characterization. Specifically, the lack of a minimum principle of trajectories forestalls the application of relaxation, gamma convergence, and other methods of the calculus of variations to the determination of the effective energetics and kinetics of systems exhibiting evolving microstructures.

Mielke and Ortiz [22] have proposed a class of variational principles for trajectories that addresses this difficulty. The fundamental idea is to *string together* the minimum problems (2.2.4c) for different times into a single minimum principle. In order to ensure causality, the rate problems corresponding to earlier times are given overwhelmingly more weight than the rate problems corresponding to later times. This leads to the consideration of the family of functionals

$$F_\epsilon(u) = \int_0^T e^{-t/\epsilon} G(t, u(t), \dot{u}(t)) dt \quad (2.2.7)$$

and to the minimum principles

$$\inf_{u \in X} F_\epsilon(u) \quad (2.2.8)$$

where X is a space of functions from $(0, T)$ to Y , or *trajectories*, such that $u(0) = u_0$. We shall refer to F_ϵ as the *energy-dissipation functional* to acknowledge the fact that F_ϵ accounts for both the energetics and the dissipation characteristics of the system. For additive problems of the form (2.2.5), an alternative form of the energy dissipation functional can be obtained through an integration by parts of the dissipation term, with the result

$$F_\epsilon(u) = \int_0^T e^{-t/\epsilon} \left[\Psi(\dot{u}) + \frac{1}{\epsilon} E(u) \right] dt \quad (2.2.9)$$

up to inconsequential additive constants.

That the *causal limit* $\epsilon \rightarrow 0$ of (2.2.8) is equivalent to problem (2.2.4) can be established formally from the Euler-Lagrange equations of F_ϵ . Thus, the Euler-Lagrange equation of (2.2.4c) is, simply,

$$\partial_v G(t, u, v) = 0 \quad (2.2.10)$$

whereas the Euler-Lagrange equations of (2.2.8) are:

$$\partial_{\dot{u}} G(t, u(t), \dot{u}(t)) + \epsilon \left\{ \partial_u G(t, u(t), \dot{u}(t)) - \frac{d}{dt} \partial_{\dot{u}} G(t, u(t), \dot{u}(t)) \right\} = 0 \quad (2.2.11)$$

A comparison of (2.2.10) and (2.2.11) reveals that, disregarding higher-order terms in ϵ , the minimizers $u(t)$ of (2.2.8) are such that $\dot{u}(t)$ solves the rate problem (2.2.4c) at all times. The Euler-Lagrange equation (2.2.11) may also be regarded as an *elliptic regularization* of problem (2.2.4) [22]. Thus, depending on the size of ϵ the system is allowed to *peep* into the future to a greater or lesser extent. In the same manner as the term *rate problem* is used to denote the problem that determines rates, namely problem (2.2.4c), we shall use the term *trajectory problem* to refer to the problem that determines the trajectories of the systems, namely problem (2.2.8).

A class of problems that is amenable to effective analysis concerns *rate-independent systems* for which the dissipation potential Ψ is homogeneous of degree 1 [22]. A striking first property of rate-independent problems is that all minimizers u^ϵ of F_ϵ satisfy energy balance independently of the value of ϵ . Under suitable coercivity assumptions it is then possible to derive *a priori* bounds for u^ϵ which likewise are independent of ϵ , with the result that it is possible to extract convergent subsequences and find limiting functions u . Under certain regularity assumptions it follows that all such limits satisfy the *energetic formulation* of Mielke *et al.* (see, e. g., the survey [21] and references therein) for rate-independent systems of the form (2.2.5). Moreover, if $(\Psi_k)_{k \in \mathcal{N}}$ converges to Ψ and E_k Γ -converges to E with respect to appropriate topologies, then the accumulation points of the family $(u_{\epsilon,k})_{\epsilon > 0, k \in \mathcal{N}}$ for $\epsilon, 1/k \rightarrow 0$ solve the associated limiting energetic formulation. These results for rate-independent systems provide a first indication that the variational program outlined above indeed works, i. e., that the minimizers of the energy-dissipation functionals F_ϵ converge towards trajectories of the evolutionary problem. The case of a general rate functional G remains open at present.

2.3 Fracture mechanics as a rate problem

Fracture is irreversible, dissipative and is driven by energetic driving forces, which suggests that it should be describable within the energy-dissipation framework outlined in the preceding section. However, whereas the energy of a body undergoing fracture is simply given by its elastic energy, the dissipation attendant to crack growth is concentrated on the crack front and its proper accounting requires carefully crafted measure-theoretical tools. Before embarking on the development of those tools, we begin by briefly recounting the elements of formal fracture mechanics that lead to the formulation of dissipation potentials for growing cracks. We therefore proceed formally and

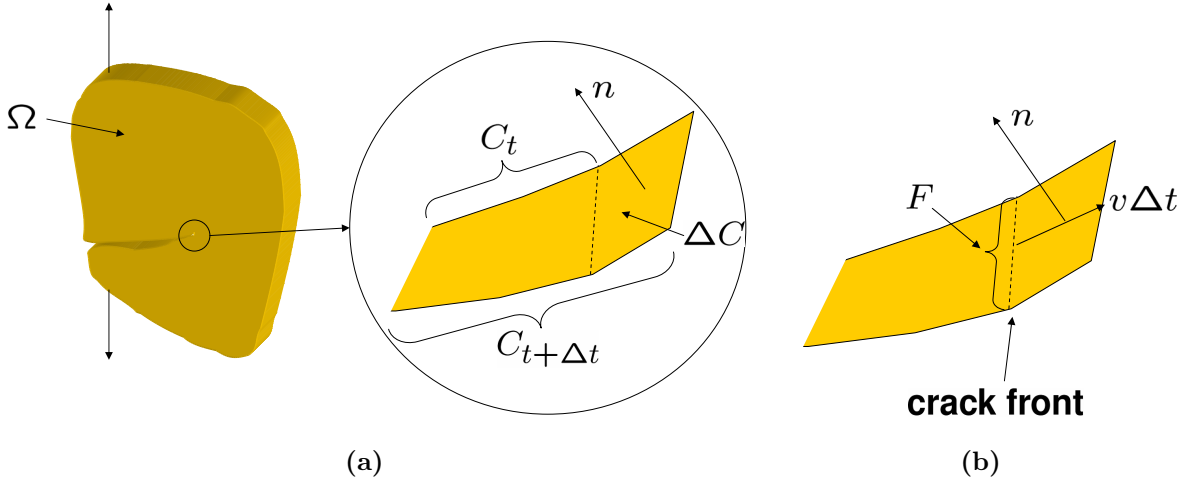


Figure 2.1: a) Crack advancing in a body occupying domain Ω and zoom of the crack-front region showing crack set C_t at time t , contained with crack set $C_{t+\Delta t}$ at time $t+\Delta t$, during which interval of time the crack front sweeps an area ΔC of unit normal n . b) Detail of advancing front and definition of front velocity.

assume regularity and smoothness as required.

We consider an elastic body occupying a domain $\Omega \subset \mathbb{R}^N$, $N \geq 2$. The boundary $\partial\Omega$ of the body consists of an exterior boundary Γ , corresponding to the boundary of the uncracked body, and a collection of cracks jointly defining a crack set C . In addition, Γ partitions in the usual manner into a displacement boundary Γ_1 and a traction boundary Γ_2 . The body undergoes deformations under the action of body forces, displacements prescribed over Γ_1 and tractions applied over Γ_2 . Under these conditions, the elastic energy of the body is

$$E(u) = \int_{\Omega} W(x, u, \nabla u) dx + \int_{\Gamma_2} V(x, u) d\mathcal{H}^{N-1} \quad (2.3.12)$$

where dx is the N -dimensional Lebesgue measure, \mathcal{H}^d is the d -dimensional Hausdorff measure, W is the elastic strain energy density of the body and V is the potential of the applied tractions. Suppose now that the applied loads and prescribed displacements are incremented over the time interval $[t, t + \Delta t]$ and that, in response to this incremental loading, the crack set extends from $C(t)$ to $C(t + \Delta t)$. Owing to the irreversibility of fracture we must necessarily have that $C(t) \subset C(t + \Delta t)$. The elastic energy released

during the time increment is

$$\begin{aligned} -\Delta E = & \left[\int_{\Omega} W(x, u(t), \nabla u(t)) dx + \int_{\Gamma_2} V(x, u(t)) d\mathcal{H}^{N-1} \right] \\ & - \left[\int_{\Omega} W(x, u(t + \Delta t), \nabla u(t + \Delta t)) dx + \int_{\Gamma_2} V(x, u(t + \Delta t)) d\mathcal{H}^{N-1} \right]. \end{aligned} \quad (2.3.13)$$

Expanding to first order in all incremental terms we obtain

$$-\Delta E \sim - \left[\int_{\Omega} (\partial_u W \cdot \Delta u + \partial_{\nabla u} W \cdot \nabla \Delta u) dx + \int_{\Gamma_2} \partial_u V \cdot \Delta u d\mathcal{H}^{N-1} \right]. \quad (2.3.14)$$

Integrating by parts and using the equations of equilibrium this expression reduces to

$$-\Delta E \sim \int_{\Delta C} T(t) \cdot [u(t + \Delta t)] d\mathcal{H}^{N-1} \quad (2.3.15)$$

where

$$T = \partial_{\nabla u} W(x, u, \nabla u) n \quad (2.3.16)$$

are the internal tractions, with n the unit outward normal to the boundary, and we write $\Delta C = C(t + \Delta t) \setminus C(t)$, Fig. 2.1a. The corresponding energy release rate now follows as

$$-\dot{E} = - \lim_{\Delta t \rightarrow 0} \frac{\Delta E}{\Delta t} = \int_F f(n) v d\mathcal{H}^{N-2} \quad (2.3.17)$$

where F is the crack front, Fig. 2.1b, v is the crack-front velocity

$$f(n) = \lim_{\Delta t \rightarrow 0} \frac{1}{\Delta t} (\partial_{\nabla u} W n) \cdot [u_{t+\Delta t}] \quad (2.3.18)$$

is the energetic force acting on the crack front. The identity (2.3.17) expresses the rate at which energy flows to—and is subsequently dissipated at—the crack front. In particular, the duality-pairing structure of (2.3.17) is conventionally taken to mean that the energetic force $f(n)$ does power, or *drives* on the crack-front velocity v . On this basis, it is customary in fracture mechanics to postulate the existence of a *crack-tip equation of motion* of the form

$$f = \partial\psi(v) \quad (2.3.19)$$

where ψ is a dissipation potential density per unit crack-front length. The total dissipa-

tion potential for the entire crack front finally follows by additivity as

$$\Psi(v) = \int_F \psi(v) d\mathcal{H}^{N-2} \quad (2.3.20)$$

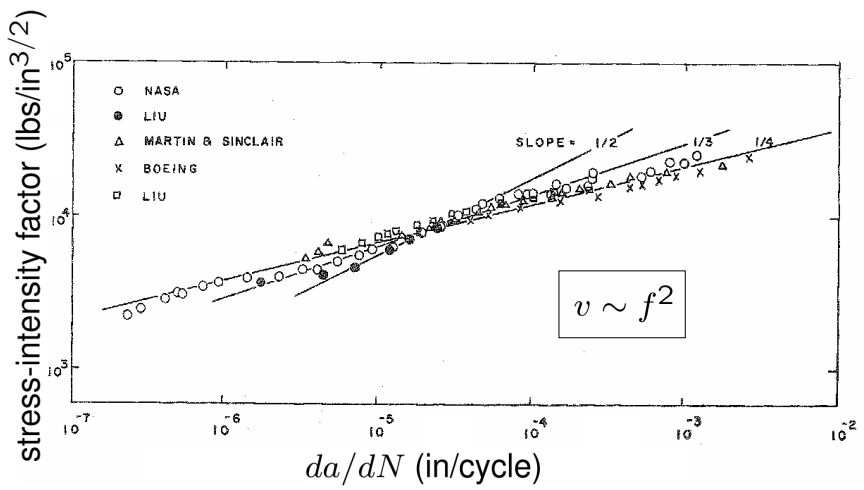
We note that constitutive relations of the form (2.3.19) can also be derived—instead of just postulated—from (2.3.17) and the first and second laws of thermodynamics using Coleman and Noll’s method [10]. The crack-tip equation of motion (2.3.19) is subject to the dissipation inequality

$$f \cdot v \geq 0 \quad (2.3.21)$$

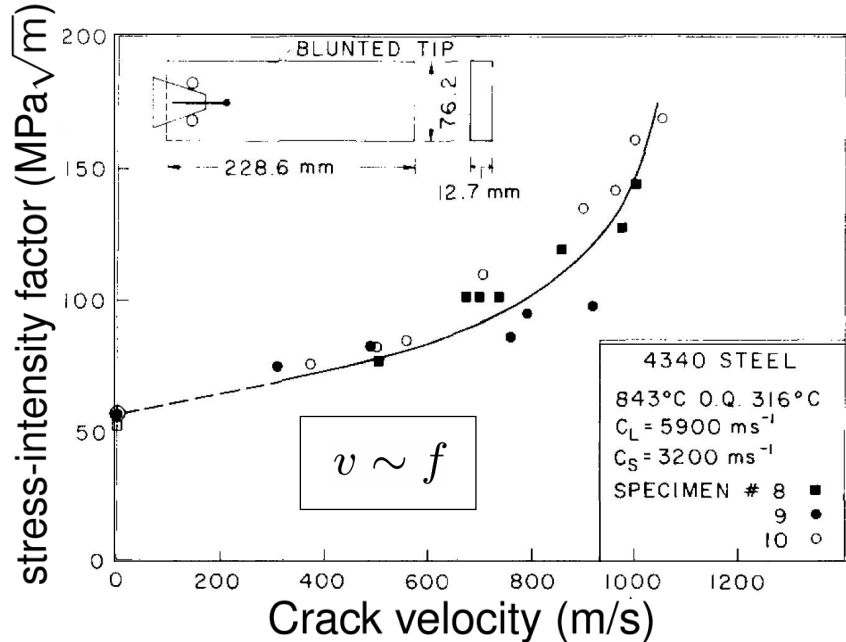
which follows as a consequence of the second law of thermodynamics. In the present context, the dissipation inequality introduces a unilateral constraint that prevents crack healing.

We note that the dissipation attendant to crack growth is localized to the crack front F , which is a set of co-dimension 2. This is in contrast to energetic theories of fracture based on the SBV or SBD formalisms in which the principal singular set of interest, namely, the crack set, has co-dimension 1. In geometrical measure theory the structure and properties of sets of co-dimension 2 is less well understood than those of sets of co-dimension 1, which adds difficulty to the energy-dissipation version of fracture mechanics. We also note that in rate-independent theories of fracture mechanics the dissipation is described by a surface energy on the crack flanks and lumped together with the energy.

The observational record lends support to the assumption that crack growth obeys a crack-tip equation of motion of the form (2.3.19). By way of example, Fig. 2.2 shows a compilation of fatigue data for 2024-T3 aluminum alloy from the classical work of Paris and Erdogan [24] and dynamic fracture data for 4340 steel [25]. In the case of fatigue, the number N of loading cycles plays the role of time. In interpreting these data it should also be recalled that in linear-elastic fracture mechanics the driving force f scales as the square of the stress-intensity factor. By plotting the driving force *vs.* crack-tip velocity on log-log axes, all the data points ostensibly collapse on master curves suggesting the existence of a crack-tip equation of motion. The data displayed in Fig. 2.2 is also suggestive of power-law behavior, possibly with a threshold on the driving force. Thus, with the direction of advance prescribed, e. g., by symmetry, the component of the crack-tip equation of motion normal to the front within the tangent plane to the



(a)



(b)

Figure 2.2: a) Compilation of fatigue data for 2024-T3 aluminum alloy [24] b) Dynamic fracture data for 4340 steel [25]. The driving force f scales as the square of the stress-intensity factor. By plotting the driving force *vs.* crack-tip velocity on log-log axes, all the data points collapse on master curves.

crack takes the form

$$v = C(f - f_0)^m \quad (2.3.22)$$

where the threshold $f_0 \geq 0$, C and m are material constants. If the rate of dissipation is further assumed to be independent of the direction of crack advance, then the dissipation potential follows as

$$\psi(v) = f_0|v| + \frac{mC}{m+1}|v|^{1+1/m} \quad (2.3.23)$$

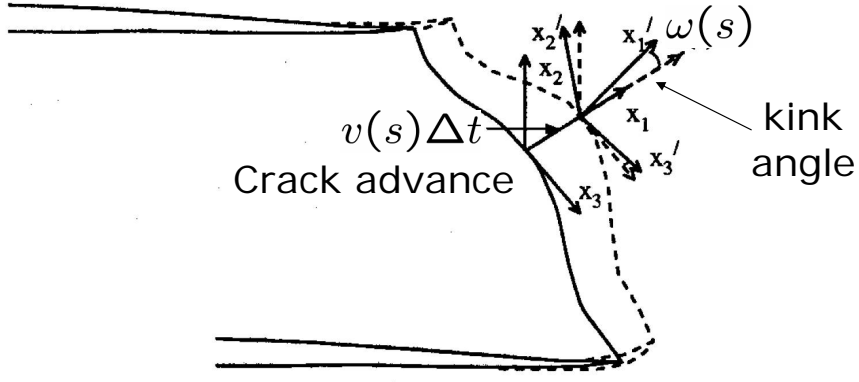


Figure 2.3: Local view of the geometry and kinetics of crack advance.

We are now in a position to formulate the *rate problem* (2.2.5) for fracture mechanics. In view of identity (2.3.17), the rate problem of fracture mechanics reduces to

$$\inf_{v,n} \int_F [\psi(v) - f(n) \cdot v] d\mathcal{H}^{N-2} \quad (2.3.24)$$

and the corresponding Euler-Lagrange equations are

$$\partial\psi(v) = f(n) \quad (2.3.25a)$$

$$\partial\psi^*(f(n)) = 0 \quad (2.3.25b)$$

which jointly determine the crack-tip velocity v and direction of advance n . The resulting geometry and kinetics of crack advance is illustrated in Fig. 2.3, that represents a local neighborhood of the crack front, e. g., parametrized by its arc length s , with the local crack geometric described by orthonormal axes tangent to the crack and its front. Because of the constraint $C(t) \subset C(t + \Delta t)$, it follows that the direction of crack

advance can locally be described by means of a single *kinking angle* $\omega(s)$. Also, because of the constraint (2.3.25b) reduces to one single equation for the determination of $\omega(s)$. We note from (2.3.24) that the resulting kinking angle maximizes the energy-release rate or, equivalently, the rate of dissipation $f(n) \cdot v$, and thus we can regard (2.3.24) variously as a maximum energy-release or a maximum dissipation principle. Once $\omega(s)$, and by extension $n(s)$, is determined from (2.3.25b) the local crack-front velocity $v(s)$, giving the rate of extension of the crack, follows from (2.3.25a), which simply restates the crack-tip equation of motion.

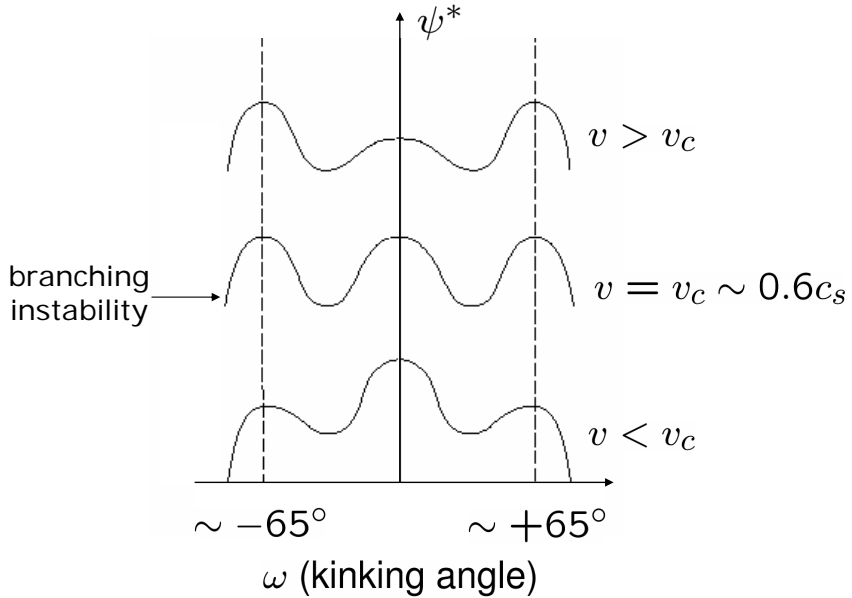


Figure 2.4: Dual dissipation density as a function of kinking angle for steady-state dynamic crack growth at different crack tip velocities. The dual energy-dissipation density has a single maximum below a critical crack-tip velocity, corresponding to straight-ahead growth, and two maxima above the critical speed [29].

The energy-dissipation functional (2.3.24) can exhibit complex behavior. A case in point is furnished by a dynamic two-dimensional crack propagating in a steady state. In this case, an equivalent static problem can be obtained by introducing a reference frame that moves with the crack tip, and the equivalent static problem thus defined can be analyzed within the energy-dissipation framework just outlined. A classical solution of Yoffe [29] then shows that for crack-tip velocities below a certain critical speed v_c of the order of 60% of the shear wave speed (2.3.25b) has a single solution and the crack runs straight ahead. By way of sharp contrast, above the critical speed (2.3.25b) has two symmetrical solutions corresponding to kinking angles of the order of $\pm 65^\circ$ corresponding to *crack branching*. In the present variational framework, this classical branching instability of dynamic fracture can thus be understood as a consequence of the lack of convexity of the rate problem, which furnishes a new insight into the phenomenon and opens opportunities for the analysis of crack branching.

On the basis of preceding description of the energetics and dissipation of fracture we

can now exhibit the energy dissipation functional (2.2.9) of fracture mechanics, namely,

$$F_\epsilon(u) = \int_0^T e^{-t/\epsilon} \left[\int_F \psi(v) d\mathcal{H}^{N-2} + \frac{1}{\epsilon} \left(\int_\Omega W(x, u, \nabla u) dx + \int_{\Gamma_2} V(x, u) d\mathcal{H}^{N-1} \right) \right] dt. \quad (2.3.26)$$

Minimization of this energy-dissipation functional supplies the entire crack-path over the time interval $[0, T]$ and the attendant trajectory of the displacement field. The energy-dissipation functional (2.3.26) forms the basis of the analysis presented in the remainder of the paper.

Remark 2.3.1. *We close this section by noting that this front-based variational model can also be used in the discrete-time incremental approach, by considering for crack increments ΔC in the time interval $[t_1, t_2]$ the crack energy*

$$\inf \left\{ \liminf_{n \rightarrow \infty} \int_{t_1}^{t_2} \int_{F_n} \psi(v_n) d\mathcal{H}^{N-2} dt : C_n \rightarrow \Delta C \right\}$$

where F_n is the front corresponding to C_n and the convergence $C_n \rightarrow \Delta C$ is in the sense described in Section 2.6. Remarkably, as a consequence of the results in that section (see Remark 2.6.11 and Theorem 2.6.12), this inf is simply

$$\inf \left\{ \liminf_{n \rightarrow \infty} \int_{t_1}^{t_2} \int_{F_n} \mathcal{C} v_n d\mathcal{H}^{N-2} dt : C_n \rightarrow \Delta C \right\} = \mathcal{CH}^{N-1}(\Delta C), \quad (2.3.27)$$

where

$$\mathcal{C} := \inf_{s \in (0, \infty)} \frac{\psi(s)}{s}.$$

2.4 Notation and mathematical setting

We first introduce some notation to be used throughout this chapter, which is consistent with [15].

- Ω , a bounded open subset of \mathbb{R}^N with Lipschitz boundary, represents the reference configuration of the body. As a mechanism for enforcing boundary conditions (see for instance [16]), Ω' will denote a bounded open set with Lipschitz boundary such that $\Omega \subset\subset \Omega'$.
- For $y \in \mathbb{R}^N$, let (y^1, \dots, y^N) denote the components of y .

- For $n = 0, \dots, N$ \mathcal{L}^n is the n -dimensional Lebesgue measure and \mathcal{H}^n denotes the n -dimensional Hausdorff measure.
- $SBV(\Omega)$ is the space of *special functions of bounded variation on Ω* . For $u \in SBV(\Omega)$, we will denote the approximate discontinuity set of u as $S(u)$ (see [4]). $SBV_p(\Omega)$ will denote those $u \in SBV(\Omega)$ such that $\nabla u \in L^p(\Omega)$.
- We will say that a sequence $\{v_n\}_{n=1}^\infty \subset SBV(\Omega)$ converges to $v \in SBV(\Omega)$ (or $v_n \xrightarrow{SBV} v$) if

$$\left\{ \begin{array}{l} \nabla v_n \rightharpoonup \nabla v \text{ in } L^1(\Omega); \\ [v_n]_{\nu_n} \mathcal{H}^{N-1}|S(v_n) \xrightarrow{*} [v]_{\nu} \mathcal{H}^{N-1}|S(v) \text{ as measures;} \\ v_n \rightarrow v \text{ in } L^1(\Omega); \text{ and} \\ v_n \xrightarrow{*} v \text{ in } L^\infty(\Omega), \end{array} \right.$$

where ν denotes the normal to $S(v)$, and $[v]$ the jump of v . Note that, as a consequence (see [2]),

$$\mathcal{H}^{N-1}(S(v)) \leq \liminf_{n \rightarrow \infty} \mathcal{H}^{N-1}(S(v_n)) \quad (2.4.28)$$

whenever $v_n \xrightarrow{SBV} v$.

- For any set of finite perimeter E , $\partial^* E$ denotes the reduced boundary of E , and for $x \in \partial^* E$, $\nu_E(x)$ denotes the measure theoretic outer normal to E at x .
- For $\xi \in \mathbb{R}$, let E_ξ^w denote the ξ super level set of w , i.e., $E_\xi^w := \{x \in \Omega : w(x) > \xi\}$.
- For $\{K_i\}_{i=1}^\infty$, $K_i \subset \mathbb{R}^2$, we use the notation $K = \underset{i \rightarrow \infty}{\text{H-lim}} K_i$ or $K_i \xrightarrow{H} K$ to mean that K_i converges to K in the Hausdorff metric.
- $A \tilde{\subset} B$ means that $\mathcal{H}^{N-1}(A \setminus B) = 0$. $A \tilde{\equiv} B$ means $\mathcal{H}^{N-1}(A \Delta B) = 0$.
- 2^X denotes the power set of X .
- $Q(x, r)$ is a cube in \mathbb{R}^N centered at x with side length $2r$.
- $B(x, r)$ is a closed ball centered at x with radius r .

- $W : \mathbb{R}^N \rightarrow \mathbb{R}$ is convex with minimum attained for $\xi \in \mathbb{R}^N$ with $\|\xi\|_{\mathbb{R}^N} = 0$ and satisfies $C_1|\xi|^p - \frac{1}{C_1} \leq W(\xi) \leq C_2(|\xi|^p + 1)$ for some positive constants C_1, C_2 and some $p > 1$.

2.5 Existence for constrained trajectories

In this section, we present an existence result for a constrained version of the problem that we introduced in Section 2.1. We are restricting our consideration to the two dimensional case ($\Omega \subset \mathbb{R}^2$), and, motivated by the compactness issues for the class of trajectories that satisfy (2.1.1) (see Section 2.1), we define a class of *constrained* trajectories:

Definition 2.5.1. *For fixed $p' > 0$, the class $\mathcal{T}_{p'}$ is the set of triples (u, C, F) such that:*

1. u satisfies:

- (a) $u(\cdot, t) \in SBV_p(\Omega') \quad \forall t \in [0, T]$
- (b) $\int_{\Omega} W(\nabla u(x, \cdot)) dx \in L^1([0, T]; \mathbb{R})$
- (c) $\forall t \in [0, T], u(\cdot, t) = g$ on $\Omega' \setminus \bar{\Omega}$, where $g \in L^\infty(\Omega') \cap H^1(\Omega')$ is given.

2. $C : [0, T] \rightarrow \{K \subset \bar{\Omega} : K \text{ is } \mathcal{H}^1 \text{ measurable}, \mathcal{H}^1(K) < \infty\}$ such that:

- (a) $C(0) \overset{\sim}{=} C_0$, for given closed C_0
- (b) C nondecreasing: $\forall \tau < t, C(\tau) \overset{\sim}{\subset} C(t)$
- (c) $\forall t \in [0, T], S(u(t)) \overset{\sim}{\subset} C(t)$
- (d) $F \in W^{1,p'}([0, T]; \bar{\Omega})$, and there exists a family of functions $v(\cdot, t) : F(t) \rightarrow \mathbb{R}$, such that
$$\int_0^T \dot{\varphi}(t) \int_{C(t)} f(x) d\mathcal{H}^1(x) dt = - \int_0^T \varphi(t) \int_{F(t)} f(x) v(x, t) d\mathcal{H}^0(x) dt$$

$$\forall \varphi \in C_0^1([0, T]), \forall f \in C_0(\Omega').$$

Property 2 expresses the fact that we are considering a relaxed definition of crack set, as discussed in the introduction. By Property 2d, we are only considering those trajectories that satisfy the front representation, and further that their fronts are at most one point $\forall t \in [0, T]$ with no jumps in the position of this front. Since the class

of trajectories that have a one point front moving continuously is not closed, we allow the front point to move inside of the existing crack set (with $v = 0$). Therefore, we can choose $F \in W^{1,p'}([0, T], \bar{\Omega})$ such that at every $t \in [0, T]$, the front at time t is a subset of $F(t)$. We will consider a dissipation potential of a similar character to that of (23) in [19], in particular we require superlinear growth of the dissipation potential. However, since F can move inside of the existing crack set, a sequence $\{q_i\}_{i=1}^\infty \subset \mathcal{T}_{p'}$ will have a subsequence that converges to an element of $\mathcal{T}_{p'}$ only if $\sup_i \|\dot{F}_i\|_{L^{p'}}^p$ is bounded, and therefore, in order to ensure compactness, we must penalize the derivative of F in the functional. Accordingly, we will minimize

$$I_{\epsilon, p'}[q] := \int_0^T e^{-\frac{t}{\epsilon}} \left\{ \frac{1}{\epsilon} \int_\Omega W(\nabla u(x, t)) dx + \int_{F(t)} |\dot{F}|^{p'}(t) d\mathcal{H}^0(x) \right\} dt$$

over $q = (u, C, F) \in \mathcal{T}_{p'}$, where $\epsilon > 0$ and $p' > 1$ are fixed. Note that the proof of Theorem 2.5.2 below applies to all convex potentials with p' growth, in particular for $|\dot{F}| + |\dot{F}|^{p'}$, as in (23) of [19]. Since $F(t)$ is only one point, the energy is simply

$$I_{\epsilon, p'}[q] := \int_0^T e^{-\frac{t}{\epsilon}} \left\{ \frac{1}{\epsilon} \int_\Omega W(\nabla u(x, t)) dx + |\dot{F}|^{p'}(t) \right\} dt.$$

Theorem 2.5.2. *There exists a minimizer of $I_{\epsilon, p'}$ in $\mathcal{T}_{p'}$.*

Proof. Let $\{q_i\}_{i=1}^\infty \subset \mathcal{T}_{p'}$ be a minimizing sequence for $I_{\epsilon, p'}$, meaning

$$\lim_{i \rightarrow \infty} I_{\epsilon, p'}[q_i] = \inf_{q \in \mathcal{T}_{p'}} I_{\epsilon, p'}[q].$$

This implies that

$$\sup_i \|\dot{F}_i\|_{L^{p'}([0, T]; \mathbb{R}^2)}^p < \infty. \quad (2.5.29)$$

Since $p' > 1$, then by (2.5.29), Theorem 1 in Section 4.6 of [15], and Morrey's Inequality (Theorem 3 in Section 4.5.3 of [15]) there is an $F \in W^{1,p'}([0, T]; \bar{\Omega})$ such that, up to a subsequence that we will not relabel,

$$F_i \rightarrow F \text{ in } L^\infty([0, T]; \bar{\Omega}) \text{ and} \quad (2.5.30)$$

$$\dot{F}_i \rightharpoonup \dot{F} \text{ in } L^{p'}([0, T]; \mathbb{R}^2). \quad (2.5.31)$$

Note that (2.5.31) implies:

$$\int_0^T e^{-\frac{t}{\epsilon}} |\dot{F}|^{p'}(t) dt \leq \liminf_{i \rightarrow \infty} \int_0^T e^{-\frac{t}{\epsilon}} |\dot{F}_i|^{p'}(t) dt. \quad (2.5.32)$$

Set $C(t) := C_0 \cup \bigcup_{\tau \leq t} F(\tau)$ and $\tilde{C}_i(t) := C_0 \cup \bigcup_{\tau \leq t} F_i(\tau)$. Since $F_i \rightarrow F$ uniformly then $\forall t \in [0, T] \tilde{C}_i(t) \xrightarrow{H} C(t)$. Construct $u : \Omega \times [0, T] \rightarrow \mathbb{R}$ as follows: $\forall t \in [0, T]$, take

$$u(\cdot, t) \in \operatorname{argmin} \left\{ \int_{\Omega} W(\nabla z) dx : z \in SBV(\Omega), S(z) \tilde{\subset} C(t), z = g \text{ in } \Omega' \setminus \Omega \right\}, \quad (2.5.33)$$

which is nonempty by the properties of W and the compactness of the space SBV (Theorems 4.7 and 4.8 of [4]).

Let $q := (u, C, F)$ as defined above. We will now show that $q \in \mathcal{T}_{p'}$, and that it is a minimizer of $I_{\epsilon, p'}$. First, note that properties 1a, 1c, 2a, 2b, and 2c hold for q by construction. Also, since C is nondecreasing, the map

$$t \mapsto \int_{\Omega} W(\nabla u(x, t)) dx$$

is nonincreasing, is continuous a.e. and therefore \mathcal{L}^1 measurable. This, combined with the lower semicontinuity of the bulk part of the energy means that property 1b is satisfied.

Next, we verify that the pair (C, F) satisfies property 2d of the definition of $\mathcal{T}_{p'}$. Choose a sequence $\{\eta_k\}_{k=1}^{\infty} \subset C^{\infty}([0, T]; \bar{\Omega})$ such that $\eta_k \rightarrow F$ strongly in $W^{1,p'}([0, T]; \bar{\Omega})$ (see Section 4.2 Theorem 3 of [15]). Then Morrey's Inequality (Section 4.5.3 Theorem 3 of [15]) implies

$$\eta_k \rightarrow F \text{ strongly in } L^{\infty}([0, T]; \bar{\Omega}).$$

Let $\Gamma_k(t) := \bigcup_{\tau \leq t} \eta_k(\tau)$. According to the Area formula (Theorem 1 in Section 3.3.2 in

[15]) we have $\forall k \in \mathbb{N}$ and $t < t' \in [0, T]$

$$\begin{aligned} \int_t^{t'} |\dot{\eta}_k| dt &= \int_{\bar{\Omega}} \mathcal{H}^0([t, t'] \cap \eta_k^{-1}(\{y\})) d\mathcal{H}^1(y) \\ &\geq \mathcal{H}^1(\Gamma_k(t') \setminus \Gamma_k(t)). \end{aligned} \quad (2.5.34)$$

Using the uniform convergence $\eta_k \rightarrow F$ (in particular that $\forall t \in [0, T] \Gamma_k(t) \xrightarrow{H} C(t) \setminus C_0$) and the fact that $\Gamma_k(t)$ connected, we have for all $t < t' \in [0, T]$

$$\begin{aligned} \mathcal{H}^1(C(t') \setminus C(t)) &\leq \liminf_{k \rightarrow \infty} \mathcal{H}^1(\Gamma_k(t') \setminus \Gamma_k(t)) \\ &\leq \lim_{k \rightarrow \infty} \int_t^{t'} |\dot{\eta}_k|(s) ds \\ &= \int_t^{t'} |\dot{F}|(s) ds. \end{aligned} \quad (2.5.35)$$

Using (2.5.35), we have that for any $f \in C_0(\Omega')$ and all $t < t' \in [0, T]$,

$$\begin{aligned} \left| \int_{C(t')} f d\mathcal{H}^1 - \int_{C(t)} f d\mathcal{H}^1 \right| &= \left| \int_{C(t') \setminus C(t)} f d\mathcal{H}^1 \right| \\ &\leq \|f\|_{L^\infty(\Omega')} \mathcal{H}^1(C(t') \setminus C(t)) \\ &\leq \|f\|_{L^\infty(\Omega')} \int_t^{t'} |\dot{F}|(s) ds. \end{aligned} \quad (2.5.36)$$

The estimate (2.5.36) means that, for every $f \in C_0(\Omega')$, the map

$$t \mapsto \int_{C(t)} f(x) d\mathcal{H}^1(x) \quad (2.5.37)$$

is absolutely continuous, and so there exists $D_f \in L^1([0, T]; \mathbb{R})$ such that

$$\int_0^T \dot{\varphi}(t) \int_{C(t)} f(x) d\mathcal{H}^1(x) dt = - \int_0^T \varphi(t) D_f(t) dt \quad (2.5.38)$$

for all $\varphi \in C_0^1([0, T]; \mathbb{R})$. In particular, taking $f \equiv 1$ in $\bar{\Omega}$ there is a $D \in L^1([0, T]; \mathbb{R})$ such that

$$\int_0^T \dot{\varphi}(t) \mathcal{H}^1(C(t)) dt = - \int_0^T \varphi(t) D(t) dt$$

for all $\varphi \in C_0^1([0, T]; \mathbb{R})$. Since for any $f \in C_0(\Omega')$ with $\|f\|_{L^\infty(\Omega')} \leq 1$ the map

$$t \mapsto \mathcal{H}^1(C(t)) - \int_{C(t)} f(x) d\mathcal{H}^1(x)$$

is nondecreasing, for any $f \in C_0(\Omega')$ one can show that there is a representative of D_f , denoted D_f^* , so that for all $t \in [0, T]$

$$\frac{1}{\|f\|_{L^\infty(\Omega')}} D_f^*(t) \leq D(t) < \infty$$

and for a.e. $t \in [0, T]$ the map $f \rightarrow D_f^*(t)$ is a bounded linear map on $C_0(\Omega')$. By the Riesz Representation Theorem (Theorem 1 in Section 1.8 of [15]), there exists a family of measures $\{\mu_t\}_{t \in [0, T]}$ such that for all $f \in C_0(\Omega')$

$$D_f(t) = \int_{\Omega'} f(x) d\mu_t(x) \quad (2.5.39)$$

at a.e. $t \in [0, T]$. Hence,

$$\int_0^T \dot{\varphi}(t) \int_{C(t)} f(x) d\mathcal{H}^1(x) dt = - \int_0^T \varphi(t) \int_{\Omega'} f(x) d\mu_t(x) dt, \quad (2.5.40)$$

for all $\varphi \in C_0^1([0, T]; \mathbb{R})$ and $f \in C_0(\Omega'; \mathbb{R})$. Now, we show that for a.e. $t \in [0, T]$, the measure μ_t is supported on $F(t)$. Since $F \in W^{1,p'}([0, T]; \bar{\Omega})$, $p' > 1$, F is uniformly continuous on $[0, T]$. For each $n \in \mathbb{N}$ choose $\delta_n > 0$ so that for $a, b \in [0, T]$ with $|a - b| < \delta_n$, $|F(a) - F(b)| < 1/(2n)$. Fixing an $n \in \mathbb{N}$, choose a finite set of open intervals $\{(a_k, b_k)\}_{k=1}^z$ such that

$$0 < |b_k - a_k| < \delta_n \quad \forall k,$$

and

$$\mathcal{L}^1 \left([0, T] \setminus \bigcup_k (a_k, b_k) \right) = 0.$$

Fix k and then choose some $t_k \in (a_k, b_k)$. Set

$$B := B(F(t_k), 1/(2n)).$$

For any $t \in (a_k, b_k)$, $C(t) \setminus C(a_k) \subset B$, which means

$$C(t) \setminus B = C(a_k) \setminus B$$

and so for all $f \in C_0(\Omega' \setminus B)$

$$\frac{d}{dt} (C(t) \setminus B) = 0$$

for almost every $t \in (a_k, b_k)$. Thus, by (2.5.40), for any $f \in C_0(\Omega' \setminus B)$ and almost every $t \in (a_k, b_k)$

$$\int_{\Omega'} f(x) d\mu_t(x) = 0,$$

and so for a.e. $t \in (a_k, b_k)$

$$\mu_t(\Omega' \setminus B) = 0. \quad (2.5.41)$$

By the choice of the diameter of B we know that for every $t \in (a_k, b_k)$

$$B \subset B(F(t), 1/n)$$

and so for a.e. $t \in (a_k, b_k)$

$$\begin{aligned} \mu_t(\Omega' \setminus B(F(t), 1/n)) &\leq \mu_t(\Omega' \setminus B) \\ &= 0. \end{aligned}$$

Repeating this argument for each k , and setting

$$G_n := \{t \in [0, T] : \mu_t(\Omega \setminus B(F(t), 1/n)) > 0\},$$

we have that

$$\mathcal{L}^1(G_n) = 0$$

for all $n \in \mathbb{N}$ and so the set

$$G := \{t \in [0, T] : \mu_t(\Omega \setminus F(t)) > 0\}$$

has zero measure. This means that for $t \in [0, T] \setminus G$

$$\mu_t << \mathcal{H}^0|F(t),$$

and setting

$$v(x, t) := \frac{d\mu_t}{d\mathcal{H}^0[F(t)]}(x)$$

we apply (2.5.40) to find

$$\int_0^T \dot{\varphi}(t) \int_{C(t)} f(x) d\mathcal{H}^1(x) dt = - \int_0^T \varphi(t) \int_{F(t)} f(x) v(x, t) d\mathcal{H}^0(x) dt \quad (2.5.42)$$

for all $\varphi \in C_0^1([0, T]; \mathbb{R})$ and $f \in C_0(\Omega'; \mathbb{R})$. Therefore the triple $q = (u, C, F)$ satisfies property 2d of the definition of $\mathcal{T}_{p'}$.

It remains only to show the lower semicontinuity of the bulk part of the energy. We will use this claim about our sequence u_i and the C constructed above:

Claim: Suppose that for some $w \in SBV(\Omega)$, $u_i(\cdot, t) \xrightarrow{SBV} w$. Then $S(w) \tilde{\subset} C(t)$.

Proof of Claim: Recall that $\tilde{C}_i(t) \xrightarrow{H} C(t)$. Now let $x_0 \in \Omega' \setminus C(t)$. Since $C(t)$ is closed, there exists $t^* \in [0, t]$ such that

$$D := \text{dist}(F(t^*), x_0) = \min_{s \in [0, t]} \text{dist}(F(s), x_0) > 0.$$

Set

$$B := B(x_0, D/2).$$

Then there exists $N \in \mathbb{N}$ such that $\forall i > N$

$$\tilde{C}_i(t) \cap B = \emptyset.$$

By definition of \tilde{C}_i , and since for each i the pair (C_i, F_i) satisfies the front representation formula with a front speed v_i , for any $f \in C_0(B)$ and $i > N$

$$\begin{aligned} \int_{C_i(t) \setminus C_0} f(x) d\mathcal{H}^1(x) &= \int_0^t \int_{F_i(s)} f(x) v_i(x, s) d\mathcal{H}^0(x) ds \\ &= \int_0^t \int_{F_i(s) \cap B} f(x) v_i(x, s) d\mathcal{H}^0(x) ds \\ &= 0. \end{aligned} \quad (2.5.43)$$

Then (2.5.43) implies

$$\mathcal{H}^1(C_i(t) \cap B) = 0$$

for $i > N$. By property 2c of Definition 2.5.1 we have

$$\mathcal{H}^1(S(u_i(t)) \cap B) = 0$$

for $i > N$. Therefore, applying (2.4.28) with $u_i|_B$ and $w|_B$ we have that

$$\mathcal{H}^1(S(w) \cap B) \leq \liminf_{i \rightarrow \infty} \mathcal{H}^1(S(u_i(t)) \cap B) = 0.$$

Since the above argument holds for any ball with radius less than $D/2$, and since x_0 was arbitrary, this proves the claim.

Now, to show that the bulk energy is lower semicontinuous, fix $t \in [0, T]$. Take a subsequence of $\{u_i\}_{i=1}^\infty$ such that:

$$\lim_{k \rightarrow \infty} \int_{\Omega} W(\nabla u_{i_k}(x, t)) dx = \liminf_{i \rightarrow \infty} \int_{\Omega} W(\nabla u_i(x, t)) dx.$$

We can assume, without loss of generality, that $\sup_k \|u_{i_k}(t)\|_{L^\infty} < +\infty$ since truncation merely lowers the elastic energy. By the compactness of the space of SBV (Theorem 4.8 of [4]) there exists $\bar{u}_t \in SBV(\Omega)$ such that, up to a further subsequence that we will not relabel,

$$u_{i_k} \xrightarrow{SBV} \bar{u}_t.$$

By the above claim

$$S(\bar{u}_t) \tilde{\subset} C(t),$$

and so applying the definition of u (recall (2.5.33)) we have

$$\int_{\Omega} W(\nabla u(x, t)) dx \leq \int_{\Omega} W(\nabla \bar{u}_t(x, t)) dx.$$

Therefore,

$$\begin{aligned} \int_{\Omega} W(\nabla u(x, t)) dx &\leq \int_{\Omega} W(\nabla \bar{u}_t(x, t)) dx \\ &\leq \lim_{k \rightarrow \infty} \int_{\Omega} W(\nabla u_{i_k}(x, t)) dx \\ &= \liminf_{i \rightarrow \infty} \int_{\Omega} W(\nabla u_i(x, t)) dx. \end{aligned}$$

Since the above holds for each $t \in [0, T]$, then the lower bound on W and Fatou's Lemma (see [4]) implies:

$$\begin{aligned} \int_0^T e^{-\frac{t}{\epsilon}} \int_{\Omega} W(\nabla u(x, t)) dx dt &\leq \int_0^T e^{-\frac{t}{\epsilon}} \left\{ \liminf_{i \rightarrow \infty} \int_{\Omega} W(\nabla u_i(x, t)) dx \right\} dt \\ &\leq \liminf_{i \rightarrow \infty} \int_0^T e^{-\frac{t}{\epsilon}} \int_{\Omega} W(\nabla u_i(x, t)) dx dt. \end{aligned} \quad (2.5.44)$$

Combining (2.5.32) and (2.5.44) gives

$$I_{\epsilon, p'}[q] \leq \liminf_{i \rightarrow \infty} I_{\epsilon, p'}[q_i],$$

which establishes that the triple $q = (u, C, F)$ is a minimizer of $I_{\epsilon, p'}$. \square

2.6 Relaxation and Rate-Independence

For energies of the form

$$I_{\epsilon}[q] := \int_0^T e^{-\frac{t}{\epsilon}} \left\{ \frac{1}{\epsilon} \int_{\Omega} W(\nabla u(x, t)) dx + \int_{F(t)} \psi(v(x, t)) d\mathcal{H}^{N-2}(x) \right\} dt, \quad (2.6.45)$$

(where $q \in \mathcal{T}$, $\epsilon > 0$ is fixed, and $\psi : [0, \infty) \rightarrow [0, \infty)$ is continuous) minimizing sequences can exhibit the onset of microstructures that involve the geometry of the crack front, which prevents the existence of a minimizer without strong restrictions on that geometry (see Section 2.5). In this section we will characterize the optimal crack front microstructure and prove a formula for the relaxation of the dissipation part of energies of the form (2.6.45) (see Theorem 2.6.13). This result holds in any dimension and without *a priori* constraints on the crack fronts. This section is organized as follows. Section 2.6.1 contains the definition for the appropriate class of fracture trajectories and other definitions useful for the remainder of Section 2.6. In Section 2.6.2 we describe the notion of convergence for which we prove the relaxation result- this convergence is extremely weak and thus the result of Theorem 2.6.13 holds in practical settings. Section 2.6.3 contains Theorem 2.6.13 and its proof.

2.6.1 Definitions

Definition 2.6.1. *The class \mathcal{T} is the set of pairs (u, C) such that:*

1. *u satisfies:*
 - (a) $u(\cdot, t) \in SBV_p(\Omega') \forall t \in [0, T]$
 - (b) $\int_{\Omega} W(\nabla u(x, \cdot)) dx \in L^1([0, T]; \mathbb{R})$
 - (c) $\forall t \in [0, T], u(\cdot, t) = g$ on $\Omega' \setminus \bar{\Omega}$, where $g \in L^\infty(\Omega') \cap H^1(\Omega')$ is given
2. $C : [0, T] \rightarrow \{K \subset \bar{\Omega} : K \text{ is } \mathcal{H}^{N-1} \text{ measurable, } \mathcal{H}^{N-1}(K) < \infty\}$ is such that:
 - (a) $C(0) \stackrel{\sim}{=} C_0$, for given C_0
 - (b) C nondecreasing: $\forall \tau < t, C(\tau) \stackrel{\sim}{\subset} C(t)$
 - (c) $\forall t \in [0, T], S(u(t)) \stackrel{\sim}{\subset} C(t)$
 - (d) There exists a function $F : [0, T] \rightarrow 2^\Omega$ and a family of functions $v(\cdot, t) : F(t) \rightarrow \mathbb{R}$ such that
$$\int_0^T \dot{\varphi}(t) \int_{C(t)} f(x) d\mathcal{H}^{N-1}(x) dt = - \int_0^T \varphi(t) \int_{F(t)} f(x) v(x, t) d\mathcal{H}^{N-2}(x) dt$$

$$\forall \varphi \in C_0^1([0, T]), \forall f \in C_0(\Omega').$$

Definition 2.6.2. Define the space \mathcal{T}^* to be the set of all pairs (u, C) that satisfy the properties of \mathcal{T} except for property 2d.

Remark 2.6.3. Note that an alternative to 2b in definition 2.6.1 is that v in 2d satisfies $v \geq 0$. A similar characterization is possible for $q \in \mathcal{T}^*$, requiring the weak derivative of $\mathcal{H}^{N-1}|C(t)$ to be nonnegative.

Definition 2.6.4. Define the rate independent envelope of ψ , $\bar{\psi} : [0, \infty) \rightarrow [0, \infty)$ by

$$\bar{\psi}(x) := \sup_{\substack{\phi \leq \psi \\ \phi \text{ linear}}} \phi(x).$$

And, setting

$$\mathcal{C} := \inf_{s \in (0, \infty)} \frac{\psi(s)}{s},$$

we have for $s \in [0, \infty)$

$$\bar{\psi}(s) = \mathcal{C}s.$$

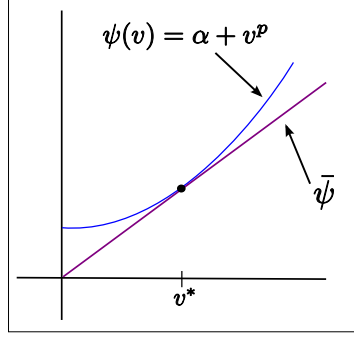


Figure 2.5: Rate-independent envelope for $\psi(v) = \alpha + v^p$, $\alpha > 0$.

2.6.2 Convergence of Trajectories

Sketch of Compactness Argument

An important feature of the choice of convergence is that minimizing sequences of (2.6.45) are compact. To motivate our choice of convergence, we will briefly sketch the compactness argument for energies of this form. Let \mathcal{D} be a countable, dense subset of $[0, T]$, and suppose that ψ has this property: there exists a constant $\mathcal{K}_1 > 0$ such that, for $s \in [0, \infty)$, ψ satisfies

$$\psi(s) \geq \mathcal{K}_1 s. \quad (2.6.46)$$

The, let $\{q_i = (u_i, C_i)\}_{i=1}^\infty \subset \mathcal{T}$ be a minimizing sequence of I_ϵ . This implies that the sequence has bounded energy, i.e., there exists $\mathcal{K}_2 > 0$ such that

$$\sup_i I_\epsilon[q_i] < \mathcal{K}_2. \quad (2.6.47)$$

We now show that there is a $q = (u, C) \in \mathcal{T}^*$ such that up to a subsequence

$$u_i(\cdot, t) \xrightarrow{SBV} u(\cdot, t)$$

for all t in the countable dense $\mathcal{D} \subset [0, T]$. To see this, we suppose that the minimizing sequence $\{q_i\}_{i=1}^\infty$ has the property that for all $i \in \mathbb{N}$ and each $t \in [0, T]$

$$u_i(\cdot, t) \in \operatorname{argmin} \left\{ \int_{\Omega} W(\nabla z) dx : z \in SBV(\Omega), S(z) \tilde{\subset} C_i(t), z = g \text{ in } \Omega' \setminus \Omega \right\},$$

since this can only reduce $I_\epsilon[q_i]$. Then, by the growth bounds on W , $\sup_{i \in \mathbb{N}} \|\nabla u_i(\cdot, t)\|_{L^p(\Omega)}$ is bounded uniformly for $t \in [0, T]$, where $p > 1$. We also assume that our minimizing sequence is chosen so that

$$\sup_{i \in \mathbb{N}} \|u_i(\cdot, t)\|_{L^\infty(\Omega')} \leq \|g\|_{L^\infty(\Omega')},$$

which, by a truncation argument, can only lower the bulk energy. Now, by (2.6.47) we have

$$\int_0^T e^{-\frac{t}{\epsilon}} \int_{F_i(t)} \psi(v_i) d\mathcal{H}^{N-2} dt < \mathcal{K}_2,$$

which combined with (2.6.46) and property 2d of the definition of \mathcal{T} means that there is a $\mathcal{K}_3 > 0$ such that

$$\begin{aligned} \mathcal{H}^{N-1}(C_i(T)) &= \int_0^T \int_{F_i(t)} v_i(x, t) d\mathcal{H}^{N-2}(x) dt \\ &< e^{-\frac{T}{\epsilon}} \mathcal{K}_3. \end{aligned} \tag{2.6.48}$$

Then, by the compactness of the space $SBV(\Omega')$ (Theorems 4.7 and 4.8 of [4]), for each $t \in \mathcal{D}$ there is an SBV function u_t such that, up to a subsequence that is not relabeled,

$$u_i(\cdot, t) \xrightarrow{SBV} u_t.$$

For $t \in \mathcal{D}$, define $u(\cdot, t) := u_t$, and since \mathcal{D} is countable, we apply a diagonal argument to show that up to a subsequence,

$$u_i(\cdot, t) \xrightarrow{SBV} u(\cdot, t) \tag{2.6.49}$$

for all $t \in \mathcal{D}$. Define, for $t \in \mathcal{D}$,

$$C(t) := \bigcup_{\substack{\tau \in \mathcal{D} \\ \tau \leq t}} S(u(\cdot, \tau)).$$

Then, one would define (u, C) suitably on $[0, T] \setminus \mathcal{D}$, so that $q = (u, C) \in \mathcal{T}^*$. Depending on the specific properties of W and ψ , this convergence can often be stronger. The proof of Theorem 2.6.13 does not depend on the strength of this convergence, thus we will use a convergence such that (2.6.49) holds on the minimal set necessary to build the limiting

crack set, giving lower semicontinuity of the energy.

Minimal Crack Trajectories

To define the convergence, we associate to each $q = (u, C) \in \mathcal{T}^*$ the *minimal crack trajectory*, C^* , by the following procedure. For each $t \in [0, T]$ set

$$\mathcal{C}_t := \left\{ K \subset \bar{\Omega} : K \text{ is } \mathcal{H}^{N-1} \text{ measurable, } S(u(\tau)) \cup C_0 \tilde{\subset} K \text{ for all } \tau \leq t \right\}, \quad (2.6.50)$$

and note that

$$\inf_{K \in \mathcal{C}_t} \mathcal{H}^{N-1}(K) \leq \mathcal{H}^{N-1}(C(T)) < \infty.$$

For each $t \in [0, T]$ take a sequence $\{C_n^t\}_{n=1}^\infty \subset \mathcal{C}_t$ such that

$$\mathcal{H}^{N-1}(C_n^t) \rightarrow \inf_{K \in \mathcal{C}_t} \mathcal{H}^{N-1}(K). \quad (2.6.51)$$

Define, for $t \in [0, T]$,

$$C^*(t) := \bigcap_{n \in \mathbb{N}} C_n^t. \quad (2.6.52)$$

Since for each $t \in [0, T]$, $C_n^t \in \mathcal{C}_t$ for every $n \in \mathbb{N}$, then

$$S(u(\tau)) \cup C_0 \tilde{\subset} C^*(t) \text{ for all } \tau \leq t \quad (2.6.53)$$

and since $C^*(t)$ is \mathcal{H}^{N-1} measurable then $C^*(t) \in \mathcal{C}_t$, which by (2.6.51) and (2.6.52) gives

$$\mathcal{H}^{N-1}(C^*(t)) = \inf_{K \in \mathcal{C}_t} \mathcal{H}^{N-1}(K) \quad (2.6.54)$$

for all $t \in [0, T]$. Note $C^*(0) \cong C_0$ and that the map

$$t \mapsto \mathcal{H}^{N-1}(C^*(t))$$

is bounded and monotone, and so is in $BV([0, T])$.

Convergence Definition

Definition 2.6.5. For $q = (u, C) \in \mathcal{T}^*$, with associated C^* , a countable set \mathcal{D} generates q if and only if for every $t \in [0, T]$

$$C^*(t) \cong C_0 \cup \bigcup_{\substack{\tau \leq t \\ \tau \in \mathcal{D}}} S(u(\tau)).$$

Lemma 2.6.6. For any $q = (u, C) \in \mathcal{T}^*$ there exists a countable dense set that generates q .

Proof. Since the map

$$t \mapsto \mathcal{H}^{N-1}(C^*(t)) \quad (2.6.55)$$

is monotone it can only have jump discontinuities, and further these jumps can only occur on a countable subset of $[0, T]$. Choose a countable dense $\mathcal{D}^* \subset [0, T]$ that contains all of the times where the map in (2.6.55) has a jump discontinuity. Define, for $t \in [0, T]$ and any countable dense $\mathcal{D} \subset [0, T]$,

$$C(\mathcal{D}, t) := C_0 \cup \bigcup_{\substack{\tau \leq t \\ \tau \in \mathcal{D}}} S(u(\tau)).$$

Then, for each $t \in \mathcal{D}^*$ take a sequence of countable dense subsets $\{\mathcal{D}_n^t\}_{n=1}^\infty$ such that

$$\mathcal{H}^{N-1}(C(\mathcal{D}_n^t, t)) \rightarrow \sup_{\mathcal{D}'} \mathcal{H}^{N-1}(C(\mathcal{D}', t)) < \infty.$$

Now, set

$$\mathcal{D}_t := \bigcup_{n \in \mathbb{N}} \mathcal{D}_n^t.$$

Since \mathcal{D}_t is countable and dense then

$$\mathcal{H}^{N-1}(C(\mathcal{D}_t, t)) = \sup_{\mathcal{D}'} \mathcal{H}^{N-1}(C(\mathcal{D}', t)).$$

Then, set

$$\mathcal{D} := \bigcup_{t \in \mathcal{D}^*} \mathcal{D}_t,$$

and so at each $t \in \mathcal{D}^*$ we have

$$\mathcal{H}^{N-1}(C(\mathcal{D}, t)) = \sup_{\mathcal{D}'} \mathcal{H}^{N-1}(C(\mathcal{D}', t)). \quad (2.6.56)$$

\mathcal{D} is a countable dense subset of $[0, T]$, and we will now show that it generates q . First, let $t \in \mathcal{D}^*$. From (2.6.53) we have

$$C(\mathcal{D}, t) \tilde{\subset} C^*(t). \quad (2.6.57)$$

For any $t_0 \leq t$,

$$\mathcal{H}^{N-1}(S(u(t_0)) \setminus C(\mathcal{D}, t)) = 0,$$

since otherwise the countable dense subset $\mathcal{D} \cup \{t_0\}$ would contradict (2.6.56). Then since $C(\mathcal{D}, t)$ is \mathcal{H}^{N-1} measurable it is in \mathcal{C}_t and by (2.6.54)

$$\mathcal{H}^{N-1}(C^*(t)) \leq \mathcal{H}^{N-1}(C(\mathcal{D}, t)).$$

Combining with (2.6.57) we have for $t \in \mathcal{D}^*$

$$C^*(t) \tilde{\equiv} C(\mathcal{D}, t). \quad (2.6.58)$$

Now take $t \in [0, T] \setminus \mathcal{D}^*$. Choose an increasing sequence $\{t_k\}_{k=1}^\infty \subset \mathcal{D}^*$ such that $t_k \rightarrow t$. Since

$$\begin{aligned} \bigcup_{k \in \mathbb{N}} C^*(t_k) &\tilde{\equiv} \bigcup_{k \in \mathbb{N}} C(\mathcal{D}, t_k) \\ &\tilde{\equiv} \bigcup_{\substack{\tau < t \\ \tau \in \mathcal{D}}} S(u(\tau)), \end{aligned} \quad (2.6.59)$$

then by (2.6.53)

$$\bigcup_{k \in \mathbb{N}} C^*(t_k) \tilde{\subset} C(\mathcal{D}, t) \tilde{\subset} C^*(t). \quad (2.6.60)$$

Therefore

$$\mathcal{H}^{N-1}\left(\bigcup_{k \in \mathbb{N}} C^*(t_k)\right) \leq \mathcal{H}^{N-1}(C(\mathcal{D}, t)) \leq \mathcal{H}^{N-1}(C^*(t)). \quad (2.6.61)$$

By (2.6.59) the sequence $\{C^*(t_k)\}_{k=1}^\infty$ is nondecreasing and so by choice of the set \mathcal{D}^*

$$\begin{aligned}\mathcal{H}^{N-1}\left(\bigcup_{k \in \mathbb{N}} C^*(t_k)\right) &= \lim_{k \rightarrow \infty} \mathcal{H}^{N-1}(C^*(t_k)) \\ &= \mathcal{H}^{N-1}(C^*(t)).\end{aligned}$$

Combining this with (2.6.60) and (2.6.61) gives

$$C^*(t) \cong C(\mathcal{D}, t).$$

Therefore the set \mathcal{D} generates q . \square

Definition 2.6.7. We will say that $q_i \rightarrow q$ (with $\{q_i\}_{i=1}^\infty \subset \mathcal{T}^*$, $q \in \mathcal{T}^*$) if and only if

$$u_i(\cdot, t) \xrightarrow{SBV} u(\cdot, t) \text{ for all } t \in \mathcal{D} \quad (2.6.62)$$

for some countable dense subset \mathcal{D} that generates q .

Remark 2.6.8. Notice that if a sequence $\{q_i\}_{i=1}^\infty$ converges in \mathcal{T}^* the limit is not unique since the limiting C is not uniquely specified.

2.6.3 Relaxation Theorem

The goal of this section is to find a representation for I_ϵ^* , the relaxation of

$$I_\epsilon := \int_0^T e^{-\frac{t}{\epsilon}} \int_{F(t)} \psi(v) d\mathcal{H}^{N-2} dt$$

with the convergence in (2.6.62), i.e., for $q \in \mathcal{T}^*$

$$I_\epsilon^*[q] := \inf_{\substack{q_i \in \mathcal{T} \\ q_i \rightarrow q}} \left\{ \liminf_{i \rightarrow \infty} I_\epsilon[q_i] \right\}. \quad (2.6.63)$$

Lemma 2.6.9. The map

$$q \mapsto \int_0^T e^{-\frac{t}{\epsilon}} d\mu(t), \quad (2.6.64)$$

where $q = (u, C) \in \mathcal{T}^*$ with associated C^* and μ is the weak derivative of $t \rightarrow \mathcal{H}^{N-1}(C^*(t))$, is lower semicontinuous with the convergence (2.6.62) in \mathcal{T}^* , i.e., whenever $\{q_i\}_{i=1}^\infty \subset \mathcal{T}^*$

and $q_i \rightarrow q$ in \mathcal{T}^* , then

$$\int_0^T e^{-\frac{t}{\epsilon}} d\mu(t) \leq \liminf_{i \rightarrow \infty} \int_0^T e^{-\frac{t}{\epsilon}} d\mu_i(t).$$

Proof. Let \mathcal{D} generate q and for each $t \in \mathcal{D}$

$$u_i(\cdot, t) \xrightarrow{SBV} u(\cdot, t).$$

This implies, again for each $t \in \mathcal{D}$

$$\mathcal{H}^{N-1}(S(u(\cdot, t))) \leq \liminf_{i \rightarrow \infty} \mathcal{H}^{N-1}(S(u_i(\cdot, t))).$$

By Lemma 3.1 in [16] we then have for all $t \in [0, T]$

$$\mathcal{H}^{N-1}(C^*(t)) = \mathcal{H}^{N-1}\left(\bigcup_{\substack{\tau \leq t \\ \tau \in \mathcal{D}}} S(u(\cdot, t))\right) \leq \liminf_{i \rightarrow \infty} \mathcal{H}^{N-1}\left(\bigcup_{\substack{\tau \leq t \\ \tau \in \mathcal{D}}} S(u_i(\cdot, t))\right).$$

Denoting the minimal crack trajectories associated to q_i by C_i^* , we then have

$$\mathcal{H}^{N-1}(C^*(t)) \leq \liminf_{i \rightarrow \infty} \mathcal{H}^{N-1}(C_i^*(t)) \quad (2.6.65)$$

for any $t \in [0, T]$. Applying an integration by parts to the map in (2.6.64) gives

$$\int_0^T e^{-\frac{t}{\epsilon}} d\mu(t) = \epsilon \int_0^T e^{-\frac{t}{\epsilon}} \mathcal{H}^{N-1}(C^*(t)) dt + e^{-\frac{T}{\epsilon}} \mathcal{H}^{N-1}(C^*(T)) - \mathcal{H}^{N-1}(C_0). \quad (2.6.66)$$

Combine (2.6.65) and (2.6.66) with Fatou's Lemma and the lemma is proved. \square

We will also make use of the following lemma, which was first proved in [12] (see Lemma 4.5).

Lemma 2.6.10. Suppose $\{u_i\}_{i=1}^\infty \subset SBV_p(\Omega)$, $p > 1$, such that $\mathcal{H}^{N-1}\left(\bigcup_{i=1}^\infty S(u_i)\right) < \mathcal{C}$, for some constant \mathcal{C} . Then, $\exists v \in SBV(\Omega)$ such that

$$\bigcup_{i=1}^\infty S(u_i) \cong S(v).$$

Proof. First, we assume that for each $i \in \mathbb{N}$, $u_i \in L^\infty(\Omega)$, since for any $w \in SBV(\Omega)$, $\arctan(w) \in SBV(\Omega) \cap L^\infty(\Omega)$ and

$$S(\arctan(w)) = S(w).$$

The plan is to define a sequence $\{v_i\}_{i=1}^\infty$ by

$$v_i := \sum_{j=1}^i r_j u_j,$$

where the constants $\{r_j\}_{j=1}^\infty$ will be chosen so that three properties hold. First, $\{v_i\}_{i=1}^\infty$ will converge in SBV to some v . Also, we will have that for any $i \in \mathbb{N}$,

$$\bigcup_{j=1}^i S(u_j) \cong S(v_i).$$

Finally, we will have that for every $i \in \mathbb{N}$ there is a constant $\eta_i > 0$ such that, for all $k > i$ and $x \in S(v_k)$ (except on a set whose \mathcal{H}^{N-1} measure is less than $1/i$),

$$|[v_k](x)| > \eta_i > 0,$$

which means that the jump sets of the $\{v_i\}_{i=1}^\infty$ do not disappear in the limit. We begin by setting

$$r_1 := \frac{1}{2 \max \left\{ 1, \|\nabla u_1\|_{L^p(\Omega)} \right\} \max \left\{ 1, \|u_1\|_{L^\infty(\Omega)} \right\}}$$

and then let $v_1 := r_1 u_1$. As in [16] (see Lemma 3.1), given $\{v_j\}_{j=1}^{i-1} \subset SBV(\Omega)$, $\mathcal{H}^{N-1}(S(v_j)) < \mathcal{C} \forall j \in \mathbb{N}$, set

$$A^{i-1}(\xi) := \{x \in S(v_{i-1}) : [v_{i-1}](x) + \xi[u_i](x) = 0\},$$

where, for any $z \in SBV(\Omega)$ and $x \in S(z)$, $[z](x)$ denotes the jump in the trace from either side of $S(z)$ at x , i.e., $[z](x) := z^+(x) - z^-(x)$. Note that since the sets $A^{i-1}(\xi)$, $\xi \in \mathbb{R}$, are disjoint and measurable, $\mathcal{H}^{N-1}(A^{i-1}(\xi)) = 0$ except possibly for countably

many values of ξ . Choose $\delta_{i-1} \in (0, \delta_{i-2})$ (taking $\delta_0 := 1$) such that

$$\mathcal{H}^{N-1}(\{x \in S(v_{i-1}) : |[v_{i-1}](x)| \leq \delta_{i-1}\}) < \frac{1}{i-1}.$$

Choose $r_i \in (0, r_{i-1})$, such that

1. $r_i < \frac{\delta_{i-1}}{2^i \max \left\{ 1, \|\nabla u_i\|_{L^p(\Omega)} \right\} \max \left\{ 1, \|u_i\|_{L^\infty(\Omega)} \right\}}$ and
2. $\mathcal{H}^{N-1}(A^{i-1}(r_i)) = 0$.

Now set

$$v_i := v_{i-1} + r_i u_i = \sum_{j=1}^i r_j u_j.$$

By the choice of $\{r_i\}_{i=1}^\infty$, specifically property 2, we have that

$$S(u_j) \overset{*}{\subset} S(v_k), \quad \forall k \geq j. \quad (2.6.67)$$

Also by the choice of the $\{r_i\}_{i=1}^\infty$ (property 1), we have that

$$\begin{aligned} \|\nabla v_i\|_{L^p(\Omega)} &\leq \sum_{j=1}^i \frac{1}{2^j \max \left\{ 1, \|\nabla u_j\|_{L^p(\Omega)} \right\}} \|\nabla u_j\|_{L^p(\Omega)} \\ &\leq 1, \end{aligned} \quad (2.6.68)$$

and

$$\begin{aligned} \|v_i\|_{L^\infty(\Omega)} &\leq \sum_{j=1}^i \frac{1}{2^j \max \left\{ 1, \|u_j\|_{L^\infty(\Omega)} \right\}} \|u_j\|_{L^\infty(\Omega)} \\ &\leq 1. \end{aligned} \quad (2.6.69)$$

These two estimates, the uniform bound on $\mathcal{H}^{N-1}(S(v_i))$, and the compactness of the space $SBV(\Omega)$ (Theorems 4.7 and 4.8 of [4]) imply that there exists $v \in SBV(\Omega)$ such that, up to a subsequence,

$$[v_i] \mathcal{H}^{N-1} \lfloor S(v_i) \rightharpoonup [v] \mathcal{H}^{N-1} \lfloor S(v). \quad (2.6.70)$$

Further, by the calculation in (2.6.69), the sequence $\{v_i\}_{i=1}^\infty$ is a Cauchy sequence in L^∞ , and so converges to some $v \in L^\infty$. The uniqueness of that limit implies that the convergence in (2.6.70) holds without dropping to a subsequence. Now, by (2.6.67) we can show that

$$\bigcup_{i=1}^{\infty} S(u_i) \overset{\sim}{\subset} S(v), \quad (2.6.71)$$

by proving that

$$\bigcup_{i=1}^{\infty} S(v_i) \overset{\sim}{\subset} S(v). \quad (2.6.72)$$

So, fix $i \in \mathbb{N}$, and let $\gamma > 0$. Choose $M \in \mathbb{N}$ large enough so that $M > i$ and $1/M < \gamma$. For $k > M$,

$$S(v_i) \overset{\sim}{\subset} S(v_k), \quad (2.6.73)$$

and setting

$$B_k := \{x \in S(v_k) : |[v_k](x)| \leq \delta_k\}$$

we have, by the choice of the sequence $\{\delta_k\}_{k=1}^\infty$,

$$\mathcal{H}^{N-1}(B_k) < \gamma. \quad (2.6.74)$$

This implies that, for $x \in S(v_k) \setminus B_k$,

$$\begin{aligned} \left| \sum_{i=k+1}^{\infty} r_i[u_i](x) \right| &\leq \left| \sum_{i=k+1}^{\infty} \frac{\delta_{i-1}}{2^i \max \left\{ 1, \|u_i\|_{L^\infty(\Omega)} \right\}} 2 \|u_i\|_{L^\infty(\Omega)} \right| \\ &\leq \left| \sum_{i=k+1}^{\infty} \frac{\delta_{i-1}}{2^{i-1}} \right| \\ &\leq \left| \delta_k \sum_{i=k}^{\infty} \frac{1}{2^i} \right| \\ &< |[v_k](x)|. \end{aligned}$$

Therefore

$$S(v_k) \overset{\sim}{\subset} (B_k \cup S(v)),$$

by (2.6.74) we have

$$\mathcal{H}^{N-1}(S(v_k) \setminus S(v)) < \gamma,$$

and so (2.6.73) implies

$$\mathcal{H}^{N-1}(S(v_i) \setminus S(v)) < \gamma.$$

Since γ was arbitrary we have

$$S(v_i) \overset{\sim}{\subset} S(v),$$

and since i was arbitrary we have (2.6.72) and we have proved (2.6.71). The inclusion

$$S(v) \overset{\sim}{\subset} \bigcup_{i=1}^{\infty} S(u_i)$$

follows from (2.6.70). \square

Remark 2.6.11. Note that the rate independent envelope gives the optimal dissipation and front speed. For any $q = (u, C) \in \mathcal{T}$ and any $t_1 < t_2$, we have

$$\begin{aligned} \int_{t_1}^{t_2} \int_{F(t)} \psi(v(x, t)) d\mathcal{H}^{N-2}(x) dt &\geq \int_{t_1}^{t_2} \int_{F(t)} \bar{\psi}(v(x, t)) d\mathcal{H}^{N-2}(x) dt \\ &= \mathcal{C} \int_{t_1}^{t_2} \int_{F(t)} v(x, t) d\mathcal{H}^{N-2}(x) dt \\ &= \mathcal{C} \int_{t_1}^{t_2} \frac{d}{dt} \mathcal{H}^{N-1}(C(t)) dt \\ &= \mathcal{C} \mathcal{H}^{N-1}(C(t_2) \setminus C(t_1)). \end{aligned}$$

Also, by the continuity of ψ , there is a sequence of front speeds $\{v_i\}_{i=1}^{\infty}$ such that

$$\frac{\psi(v_i)}{v_i} \rightarrow \mathcal{C}.$$

We now show that this optimal front speed, and with it the optimal dissipation, can be achieved by using the right front geometry.

Theorem 2.6.12. Let $[a, b] \subset [0, T]$ and $\Gamma \subset \bar{\Omega}$, $\mathcal{H}^{N-1}(\Gamma) < \infty$, such that $\Gamma \cong S(w)$ for some $w \in SBV(\Omega)$. Then, for any $\delta > 0$, there is pair (C_{δ}, F_{δ}) , defined for $t \in [a, b]$, $C_{\delta}(b) \setminus C_{\delta}(a) \cong \Gamma$, the pair satisfies the properties of part 2 of Definition 2.6.1 (in particular the front representation formula with front speed that we denote v_{δ}), and

$$\int_a^b \int_{F_{\delta}(t)} \psi(v_{\delta}(x, t)) d\mathcal{H}^{N-2}(x) dt < (1 + \delta) \mathcal{C} \mathcal{H}^{N-1}(\Gamma). \quad (2.6.75)$$

Proof. The plan is to cover Γ with a countable collection of cubes so that in each cube Γ is close to a hyperplane through the center of the cube. We partition $[a, b]$ into a countable family of subintervals. In each cube we will construct (C_δ, F_δ) during one of the time subintervals by taking $N - 1$ dimensional slices of Γ that move at a speed which gives the optimal front speed, according to Remark 2.6.11 (see Figure 2.7). In each cube we will miss subsets of Γ of small \mathcal{H}^{N-1} measure, for which we later repeat the above process, and in the end we will miss only a set of \mathcal{H}^{N-1} measure zero (see Figure 2.8).

Let $A_1 = \Gamma$; in what follows we will inductively define $\{A_k\}_{k=2}^\infty$, $A_k \subset A_{k-1}$ for all $k \in \mathbb{N}$.

Part I:

First we divide $[a, b]$. Let $\{I_k\}_{k=1}^\infty$, $I_k \subset [a, b] \forall k \in \mathbb{N}$, be a countable, disjoint collection of intervals such that each I_k is nonempty and so that

$$\mathcal{L}^1 \left([a, b] \Delta \bigcup_{k=1}^\infty I_k \right) = 0.$$

Then, for each I_k , let $\{Y_\ell^k\}_{\ell=1}^\infty$, $Y_\ell^k \subset I_k \forall \ell \in \mathbb{N}$, be a countable disjoint collection of intervals, each nonempty, such that

$$\mathcal{L}^1 \left(I_k \Delta \bigcup_{\ell=1}^\infty Y_\ell^k \right) = 0.$$

So, we have that:

$$\mathcal{L}^1 \left([a, b] \Delta \bigcup_{k=1}^\infty \bigcup_{\ell=1}^\infty Y_\ell^k \right) = 0.$$

Part II:

Suppose we have defined $\{A_j\}_{j=1}^k$, with $A_j \subset A_{j-1} \subset \Gamma$ for $j = 1, \dots, k$. As outlined above, we will now cover A_k with a suitable family of cubes in order to define the crack trajectory and crack front. As in the proof of Theorem 2.1 in [16], let \mathcal{D} be a countable dense subset of \mathbb{R} such that for each $\xi \in \mathcal{D}$, E_ξ^w is a set of finite perimeter. Then

$$S(w) \underset{\xi \in \mathcal{D}}{\sim} \bigcup \partial^* E_\xi^w.$$

Let $\eta > 0$. From now on, if $x_0 \in \partial^* E$ for some specified set of finite perimeter E , assume that any cube $Q(x_0, r)$ is oriented so that $\nu_E(x_0)$ is normal to one of the faces of the cube. From [16] (see the derivation of equation (2.1) in the proof of Theorem 2.1), we know that for all $\xi \in \mathcal{D}$, and \mathcal{H}^{N-1} -a.e. $x \in A_k \cap \partial^* E_\xi^w$,

$$\lim_{r \downarrow 0} \frac{\mathcal{H}^{N-1}(Q(x, r) \cap A_k \cap \partial^* E_\xi^w)}{(2r)^{N-1}} = 1. \quad (2.6.76)$$

We have for $x \in \partial^* E_\xi^w$ (see Remark 3.55 in [4])

$$\lim_{r \downarrow 0} \int_{Q(x, r)} |\nu_{E_\xi^w}(y) - \nu_{E_\xi^w}(x)| d|D\chi_{E_\xi^w}|(y) = 0.$$

This implies that

$$\lim_{r \downarrow 0} \frac{|D\chi_{E_\xi^w}| \left(\{y \in Q(x, r) : |\nu_{E_\xi^w}(y) - \nu_{E_\xi^w}(x)| \geq \eta\} \right)}{|D\chi_{E_\xi^w}|(Q(x, r))} = 0$$

and so

$$\lim_{r \downarrow 0} \frac{|D\chi_{E_\xi^w}| \left(\{y \in Q(x, r) : |\nu_{E_\xi^w}(y) - \nu_{E_\xi^w}(x)| < \eta\} \right)}{|D\chi_{E_\xi^w}|(Q(x, r))} = 1$$

for $x \in \partial^* E_\xi^w$. Combining this with Corollary 1 of Section 5.7 in [15] we then have that, again for $x \in \partial^* E_\xi^w$,

$$\lim_{r \downarrow 0} \frac{|D\chi_{E_\xi^w}| \left(\{y \in Q(x, r) : |\nu_{E_\xi^w}(y) - \nu_{E_\xi^w}(x)| < \eta\} \right)}{(2r)^{N-1}} = 1.$$

And, since by Theorem 2 in Section 5.7 of [15] we have $|D\chi_{E_\xi^w}| = \mathcal{H}^{N-1}[\partial^* E_\xi^w]$, we have that for $x \in \partial^* E_\xi^w$

$$\lim_{r \downarrow 0} \frac{\mathcal{H}^{N-1}(Q(x, r) \cap \{y \in \partial^* E_\xi^w : |\nu_{E_\xi^w}(y) - \nu_{E_\xi^w}(x)| < \eta\})}{(2r)^{N-1}} = 1. \quad (2.6.77)$$

Combining (2.6.76) and (2.6.77), we know that for all $\xi \in \mathcal{D}$ and \mathcal{H}^{N-1} -a.e. $x \in A_k \cap$

$\partial^* E_\xi^w$,

$$\lim_{r \downarrow 0} \frac{\mathcal{H}^{N-1}(Q(x, r) \cap A_k \cap \{y \in \partial^* E_\xi^w : |\nu_{E_\xi^w}(y) - \nu_{E_\xi^w}(x)| < \eta\})}{(2r)^{N-1}} = 1. \quad (2.6.78)$$

Now, since \mathcal{D} is countable, we also have that (2.6.78) holds for \mathcal{H}^{N-1} -a.e. $x \in A_k$ and all $\xi \in \mathcal{D}$ such that $x \in \partial^* E_\xi^w$.

For \mathcal{H}^{N-1} -a.e. $x \in A_k$, we choose $\xi(x)$ such that for the set $E_x := E_{\xi(x)}^w$ we have $x \in \partial^* E_x$. We use (2.6.78) to finely cover (up to a set of \mathcal{H}^{N-1} measure zero) the set A_k with the family \mathcal{G} of all cubes $Q(x, r)$, $x \in A_k$, and r small enough so that $Q(x, r) \subset \Omega'$ and the following properties hold:

1. $(1 - \frac{\eta}{k})(2r)^{N-1} < \mathcal{H}^{N-1}(Q(x, r) \cap A_k \cap \{y \in \partial^* E_x : |\nu_{E_x}(y) - \nu_{E_x}(x)| < \eta\}) < (1 + \frac{\eta}{k})(2r)^{N-1}$
2. $(1 - \frac{\eta}{k})(2r)^{N-1} < \mathcal{H}^{N-1}(Q(x, r) \cap A_k) < (1 + \frac{\eta}{k})(2r)^{N-1}$.

Now, applying Besicovitch's Covering Theorem (specifically Corollary 1 of Section 1.5 in [15]) using the Radon measure $\mathcal{H}^{N-1}|_{A_k}$, we get a countable disjoint collection of cubes $\{Q_\ell^k\}_{\ell=1}^\infty \subset \mathcal{G}$, such that

$$\mathcal{H}^{N-1}\left(A_k \setminus \bigcup_{\ell=1}^\infty Q_\ell^k\right) = 0.$$

In each cube Q_ℓ^k , we will build up the set $A_k \cap Q_\ell^k$ in the time interval Y_ℓ^k , in a way that has a front representation, and uses the optimal front speed as calculated in Part I.

Part III:

Fix such a pair (Q_ℓ^k, Y_ℓ^k) , and we will employ the simpler notation $Y_\ell^k = [t_1, t_2]$, $\Delta t := t_2 - t_1$ and $Q_\ell^k = Q(x, r)$. Also, we assume a coordinate system so that

$$Q_\ell^k = \prod_{i=1}^N [0, 2r]$$

and $\nu_{E_x}(x) = e_1$. Define

$$G_\ell^k := Q_\ell^k \cap A_k \cap \{y \in \partial^* E_x : \nu_{E_x}^1(y) > 1 - \eta\}.$$

Note that by properties 1 and 2 of the choice of cubes we have

$$\mathcal{H}^{N-1}(Q_\ell^k \cap (A_k \setminus G_\ell^k)) < \frac{2}{k} \eta(2r)^{N-1}.$$

The plan is to define a front by taking $N - 1$ dimensional slices of the set G_ℓ^k . With this in mind, define the “slicing function” σ , which maps pairs $(t, A) \in \mathbb{R} \times \mathbb{R}^N$ to subsets of \mathbb{R}^{N-1} by

$$\sigma(t, A) := \{z \in \mathbb{R}^{N-1} : (z^1, \dots, z^{N-1}, t) \in A\}.$$

Also, define the family of imbeddings of \mathbb{R}^{N-1} into \mathbb{R}^N by setting for $t \in \mathbb{R}$ and $\tilde{A} \subset \mathbb{R}^{N-1}$:

$$\phi_t(\tilde{A}) := \left\{y \in \mathbb{R}^N : y = (z^1, \dots, z^{N-1}, t) \text{ for some } z \in \tilde{A}\right\}.$$

Set

$$S_t := \sigma(t, Q_\ell^k \cap E_x).$$

Claim:

$$\text{For } \mathcal{L}^1\text{-a.e. } t \in [0, 2r], S_t \text{ is a set of finite perimeter in } \mathbb{R}^{N-1}. \quad (2.6.79)$$

Proof of Claim: By Theorem 2 in Section 5.10 of [15], we know that $f \in BV_{\text{loc}}(\mathbb{R}^N)$ if and only if

$$\int_K (\text{ess } V_a^b f_k)(x') d\mathcal{L}^{N-1}(x') < \infty, \quad (2.6.80)$$

for each $k = 1, \dots, N$, $a < b$, and compact set $K \subset \mathbb{R}^{N-1}$, with $x' = (x_1, \dots, x_{k-1}, x_{k+1}, \dots, x_N) \in \mathbb{R}^{N-1}$ and

$$f_k(x', t) := f(\dots, x_{k-1}, t, x_{k+1}, \dots).$$

Let

$$K^* := \left(\prod_{i=1}^{N-1} [0, 2r] \right) \subset \mathbb{R}^{N-1}.$$

For any $y \in K^*$, define the function $(\chi_{E_x})_y : (0, 2r) \rightarrow \{0, 1\}$ by

$$s \mapsto (\chi_{E_x})_y(s) := \chi_{E_x \cap Q_\ell^k}(s, y).$$

Also, define the function $SV : K^* \rightarrow \mathbb{R}$ by

$$y \mapsto SV(y) := \text{ess } V_0^{2r}(\chi_{E_x})_y.$$

Since $\chi_{E_x} \in BV(\Omega)$, then applying (2.6.80), using K^* as our compact set, gives

$$\int_{K^*} SV(y) d\mathcal{L}^{N-1}(y) < \infty. \quad (2.6.81)$$

Then, if $N = 2$, we have proven (2.6.79), since for any $s, t \in (0, 2r)$, $(\chi_{E_x})_t(s) = \chi_{S_t}(s)$ and so by (2.6.81), for \mathcal{L}^1 -a.e. t , χ_{S_t} has finite essential variation. For $N > 2$, let

$$K^{**} := \left(\prod_{i=1}^{N-2} [0, 2r] \right) \subset \mathbb{R}^{N-2}.$$

Then applying Fubini's Theorem to (2.6.81) we have

$$\int_0^{2r} \int_{K^{**}} SV(y', \xi) d\mathcal{L}^{N-2}(y') d\xi < \infty.$$

So, there exists a set $\mathcal{N} \subset [0, 2r]$ such that for $\xi \in [0, 2r] \setminus \mathcal{N}$,

$$\int_{K^{**}} SV(y', \xi) d\mathcal{L}^{N-2}(y') < \infty.$$

and

$$\mathcal{L}^1([0, 2r] \setminus \mathcal{N}) = 0.$$

For any $t \in [0, 2r] \setminus \mathcal{N}$, and $y' \in K^{**}$, define the function $(\chi_{\sigma_t})_{y'} : (0, 2r) \rightarrow \{0, 1\}$ by

$$z \mapsto (\chi_{\sigma_t})_{y'}(z) := \chi_{\sigma(t, E_x \cap Q_\ell^k)}(z, y'),$$

and then define the function $SV_t : K^{**} \rightarrow \mathbb{R}$

$$y' \mapsto SV_t(y') := \text{ess } V_0^{2r}(\chi_{\sigma_t})_{y'}.$$

By definition of σ , we have that for any $t \in [0, 2r]$, $y' \in K^{**}$, and $z \in (0, 2r)$:

$$(\chi_{\sigma_t})_{y'}(z) = (\chi_{E_x})_{(y', t)}(z),$$

and so

$$SV_t(y') = SV(y', t)$$

for all $y' \in K^{**}$, $t \in [0, 2r]$. Therefore, for $t \in [0, 2r] \setminus \mathcal{N}$,

$$\int_{K^{**}} SV_t(y') d\mathcal{L}^{N-1}(y') < \infty. \quad (2.6.82)$$

Appling (2.6.82) and the other implication of Theorem 2 in Section 5.10 of [15] to the function $\chi_{\sigma(t, Q_\ell^k \cap E_x)}$ defined on \mathbb{R}^{N-1} , gives us that for \mathcal{L}^1 -a.e. $t \in [0, 2r]$, $\chi_{\sigma(t, Q_\ell^k \cap E_x)} \in BV(\mathbb{R}^{N-1})$, which means that the set S_t is a set of finite perimeter in \mathbb{R}^{N-1} , which concludes the proof of (2.6.79).

The above claim implies that there exists a set $\mathcal{N} \subset [0, 2r]$ with measure zero such that, for $t \in [0, 2r] \setminus \mathcal{N}$, there exists a vector valued Radon measure on \mathbb{R}^{N-1} , denoted

$$[\partial S_t] = (|\partial_{e_1} S_t|, \dots, |\partial_{e_{N-1}} S_t|),$$

such that

$$\int_{\sigma(t, Q_\ell^k)} \chi_{S_t}(y) \operatorname{div} \varphi(y) d\mathcal{L}^{N-1}(y) = - \int_{\sigma(t, Q_\ell^k)} \varphi(y) \cdot d[\partial S_t](y)$$

for all $\varphi \in C_0^1(\sigma(t, Q_\ell^k); \mathbb{R}^{N-1})$. And, according to Theorem 2 in Section 5.7 of [15], we have that

$$|\partial S_t| = \mathcal{H}^{N-2} |\partial^* S_t|$$

for $t \notin \mathcal{N}$.

Part IV:

The goal of this part of the proof is to show how $A_k \cap Q_\ell^k$ can be built up in a way that satisfies the front representation formula by taking a moving slice of the cube with speed 1. Define, for $t \in [0, 2r]$,

$$\tilde{F}(t) := \begin{cases} \phi_t(\sigma(t, G_\ell^k) \cap \partial^* S_t) & \text{if } t \notin \mathcal{N} \\ \emptyset & \text{if } t \in \mathcal{N} \end{cases}$$

and

$$\tilde{C}(t) := \{y \in G_\ell^k : y^N \leq t\}.$$

For every $t \in [0, 2r]$, $\tilde{C}(t)$ is the intersection of a $|D\chi_{E_x}|$ measurable set and a Borel set and therefore is $|D\chi_{E_x}|$ measurable. Also, $\tilde{C}(2r) = G_\ell^k$. To show that the pair (\tilde{C}, \tilde{F}) satisfies the front representation formula, we will define a family of measures ρ_t , $t \in [0, 2r]$, such that

$$\rho_t(A) = \int_0^t \mathcal{H}^{N-2}(\tilde{F}(\xi) \cap A) d\xi, \quad (2.6.83)$$

for any Borel set $A \subset \mathbb{R}^N$. First, we must ensure that a family of Radon measures can be defined in this manner.

For $j < N$, the measure valued map

$$t \mapsto \begin{cases} |\partial_{e_j} S_t| & \text{if } t \in [0, 2r] \setminus \mathcal{N} \\ 0 & \text{if } t \in \mathcal{N} \end{cases} \quad (2.6.84)$$

is \mathcal{L}^1 -measurable in the sense of Definition 2.25 of [4] by the following adaptation of Lemma 3.106 in [4]. By Proposition 2.6 of [4] we need to verify that for any open set $A \subset Q_\ell^k$, the map $t \mapsto |\partial_{e_j} S_t|(A)$ is \mathcal{L}^1 -measurable. Taking A to be such a set, choose a sequence $f_n \rightarrow e_j \chi_A$, $f_n \in C_0^1(A; \mathbb{R}^{N-1})$. Then, the functions

$$t \mapsto \Psi_n(t) := \int_{\sigma(t, Q_\ell^k)} \chi_{S_t}(\xi) \operatorname{div} f_n(\xi) d\mathcal{L}^{N-1}(\xi)$$

are \mathcal{L}^1 -measurable for all n by Fubini's Theorem. Since for all $n \in \mathbb{N}$

$$\int_{\sigma(t, Q_\ell^k)} \chi_{S_t}(\xi) \operatorname{div} f_n(\xi) d\mathcal{L}^{N-1}(\xi) = - \int_{\sigma(t, Q_\ell^k)} f_n(\xi) \cdot d[\partial S_t](\xi),$$

then for \mathcal{L}^1 -a.e. t ,

$$-\Psi_n(t) \rightarrow |\partial_{e_j} S_t|(A),$$

as $n \rightarrow \infty$, and so we satisfy the requirement of Proposition 2.6 of [4], which implies that the map in (2.6.84) is \mathcal{L}^1 -measurable. Further, by Theorem 3.107 in [4] we have for any $j < N$,

$$|D_{e_j} \chi_{E_x}| = \mathcal{L}^1[0, 2r] \otimes |\partial_{e_j} S_t|, \quad (2.6.85)$$

where the measure product on the right hand side is given by Definition 2.27 of [4]:

$$(\mathcal{L}^1 \llcorner [0, 2r] \otimes |\partial_{e_j} S_t|)(A) := \int_0^{2r} \int_{\sigma(t, Q_\ell^k)} \chi_{\sigma(t, A)}(\xi) d|\partial_{e_j} S_t|(\xi) dt,$$

for any $A \subset Q_\ell^k$, A Borel. Since

$$\begin{aligned} |D_{e_j} \chi_{E_x}|(Q_\ell^k) &\leq |D \chi_{E_x}|(Q_\ell^k) \\ &< \infty, \end{aligned}$$

the measure $\mathcal{L}^1 \llcorner [0, 2r] \otimes |\partial_{e_j} S_t|$ is Radon, again for $j < N$. Next, we turn our attention to the measure-valued map

$$t \mapsto \begin{cases} |\partial S_t| & \text{if } t \in [0, 2r] \setminus \mathcal{N} \\ 0 & \text{if } t \in \mathcal{N}. \end{cases} \quad (2.6.86)$$

For any $j < N$, the function ζ_j , defined for $t \in [0, 2r]$ and $x \in \prod_{i=1}^{N-1} [0, 2r]$ (up to a set of $\mathcal{L}^1 \llcorner [0, 2r] \otimes |\partial_{e_j} S_t|$ measure zero)

$$\zeta_j(t, x) := \nu_{S_t}^j(x),$$

is $\mathcal{L}^1 \llcorner [0, 2r] \otimes |\partial_{e_j} S_t|$ -measurable, and so it follows that $(\zeta_j)^2$ is $\mathcal{L}^1 \llcorner [0, 2r] \otimes |\partial_{e_j} S_t|$ -measurable. Proposition 2.26 of [4] implies that for all $j < N$, the map

$$t \mapsto \int_{\sigma(t, Q_\ell^k)} (\nu_{S_t}^j)^2(x) d|\partial S_t|(x)$$

is $\mathcal{L}^1 \llcorner [0, 2r]$ measurable, which implies that the map in (2.6.86) is $\mathcal{L}^1 \llcorner [0, 2r]$ measurable. Also, for any $j < N$,

$$\begin{aligned} \int_0^{2r} \nu_{S_t}^j(\xi) d|\partial S_t|(\xi) dt &= \int_0^{2r} |\partial_{e_j} S_t|(\sigma(t, Q_\ell^k)) dt \\ &< \infty, \end{aligned}$$

and so, since for any $t \in [0, 2r] \setminus \mathcal{N}$ and $\xi \in \mathbb{R}^{N-1}$, $\sum_{j=1}^{N-1} (\nu_{S_t}^j)^2(\xi) = 1$, we have

$$\begin{aligned} \int_0^{2r} |\partial S_t|(\sigma(t, Q_\ell^k)) dt &= \int_0^{2r} \int_{\sigma(t, Q_\ell^k)} \sum_{j=1}^{N-1} \{(\nu_{S_t}^j)^2(\xi)\} d|\partial S_t|(\xi) dt \\ &= \sum_{j=1}^{N-1} \int_0^{2r} \int_{\sigma(t, Q_\ell^k)} (\nu_{S_t}^j)^2(\xi) d|\partial S_t|(\xi) dt \\ &\leq \sum_{j=1}^{N-1} \int_0^{2r} \int_{\sigma(t, Q_\ell^k)} \nu_{S_t}^j(\xi) d|\partial S_t|(\xi) dt \\ &< \infty. \end{aligned}$$

Therefore, we define the Radon measure by the measure product

$$(\mathcal{L}^1| [0, 2r] \otimes |\partial S_t|)(A) := \int_0^{2r} \int_{\sigma(t, Q_\ell^k)} \chi_{\sigma(t, A)} d|\partial S_t|(\xi) dt,$$

for all $A \subset Q_\ell^k$, A Borel. Since the set G_ℓ^k is $|D\chi_{E_x}|$ measurable, there exists a Borel set that agrees $|D\chi_{E_x}|$ -a.e. with G_ℓ^k , and so we assume that G_ℓ^k is Borel. Therefore, we can define the family of Radon measures, $t \in [0, 2r]$, by setting for each Borel set $A \subset Q_\ell^k$

$$\begin{aligned} \rho_t(A) &:= \int_A \chi_{G_\ell^k}(y) d(\mathcal{L}^1| [0, t] \otimes |\partial S_\xi|)(y) \\ &= \int_0^t \int_{\sigma(\xi, G_\ell^k \cap A)} d|\partial S_\xi| d\xi. \end{aligned}$$

Since $|\partial S_t| = \mathcal{H}^{N-2}| \partial^* S_t$, and by definition of \tilde{F} , we can write these measures as

$$\begin{aligned} \rho_t(A) &= \int_0^t \mathcal{H}^{N-2}(\sigma(\xi, G_\ell^k \cap A) \cap \partial^* S_\xi) d\xi \\ &= \int_0^t \mathcal{H}^{N-2}(\phi_t(\sigma(\xi, G_\ell^k \cap A) \cap \partial^* S_\xi)) d\xi \\ &= \int_0^t \mathcal{H}^{N-2}(\tilde{F}(\xi) \cap A) d\xi \end{aligned} \tag{2.6.87}$$

giving (2.6.83).

Next, we show that $\forall t \in [0, 2r]$, we have that for any ball $B \subset Q_\ell^k$

$$(1 - \eta)|D\chi_{E_x}|(\tilde{C}(t) \cap B) \leq \rho_t(B) \leq |D\chi_{E_x}|(\tilde{C}(t) \cap B). \quad (2.6.88)$$

We have by choice of the set G_ℓ^k ,

$$(1 - \eta)|D\chi_{E_x}|(\tilde{C}(t) \cap B) \leq |D_{e_1}\chi_{E_x}|(\tilde{C}(t) \cap B).$$

Using (2.6.85) we have

$$\begin{aligned} |D_{e_1}\chi_{E_x}|(\tilde{C}(t) \cap B) &= \int_0^t |\partial_{e_1} S_\xi|(\sigma(\xi, \tilde{C}(t)) \cap \sigma(\xi, B)) d\xi \\ &= \int_0^t |\partial_{e_1} S_\xi|(\sigma(\xi, G_\ell^k) \cap \sigma(\xi, B)) d\xi \\ &\leq \int_0^t |\partial S_\xi|(\sigma(\xi, G_\ell^k) \cap \sigma(\xi, B)) d\xi \\ &= \int_0^t \mathcal{H}^{N-2}(\phi_\xi(\sigma(\xi, G_\ell^k) \cap \partial^* S_\xi \cap B)) d\xi \\ &= \rho_t(B), \end{aligned}$$

and so (2.6.88) is proved. This estimate implies that, $\forall t \in [0, 2r]$,

$$|D\chi_{E_x}|(\tilde{C}(t)) \ll \rho_t,$$

and that the densities

$$\gamma_t(\xi) := \frac{d(|D\chi_{E_x}|(\tilde{C}(t)))}{d\rho_t}(\xi)$$

exist $\forall t \in [0, 2r]$, ρ_t -a.e. and satisfy the uniform bounds

$$1 \leq \gamma_t \leq \frac{1}{1 - \eta}.$$

Therefore, by the generalized Fubini theorem of Definition 2.27 in [4], we have for all

$\varphi \in C_0^1([0, 2r])$ and $f \in C_0(Q(x, r))$,

$$\begin{aligned} \int_0^{2r} \dot{\varphi}(t) \int_{\tilde{C}(t)} f(x) d\mathcal{H}^{N-1}(x) dt &= \int_0^{2r} \dot{\varphi}(t) \int_{Q_\ell^k} f(x) \gamma_t(x) d\rho_t(x) dt \\ &= \int_0^{2r} \dot{\varphi}(t) \int_0^t \int_{\tilde{F}(\xi)} f(x) \gamma_\xi(x) d\mathcal{H}^{N-2}(x) d\xi dt \quad \text{by (2.6.87)} \\ &= - \int_0^{2r} \varphi(t) \int_{\tilde{F}(t)} f(x) \gamma_t(x) d\mathcal{H}^{N-2}(x) dt. \end{aligned}$$

So we see that in the cube Q_ℓ^k the pair (\tilde{C}, \tilde{F}) satisfies the front representation with front speed $v(x, t) = \gamma_t(x)$.

Part V:

Now, instead of taking single slices of the cube moving at speed of 1, we will take slices in a way that allows us to approximate the optimal front speed (this optimal slicing is illustrated in Figure 2.6 for the case where the crack increment is a square in *rn3*). By definition of \mathcal{C} , for any $\delta > 0$ we can choose $v^* \in (0, \infty)$ such that

$$\frac{\psi(v^*)}{v^*} \leq \mathcal{C}(1 + \delta).$$

Also, by the continuity of ψ , we can further take η small enough so that if $v^* < v_0 < v^* \frac{1}{1 - \eta}$ we have

$$\frac{\psi(v_0)}{v_0} \leq \mathcal{C}(1 + \delta),$$

and hence

$$\psi(v_0) \leq (1 + \delta)\mathcal{C}v_0 \quad \text{when } v^* < v_0 < v^* \frac{1}{1 - \eta}. \quad (2.6.89)$$

Set

$$l^{min} := \frac{(2r)^{N-1}}{v^* \Delta t}$$

and

$$\tilde{l} := \frac{l^{min}}{(2r)^{N-2}} = \frac{(2r)}{v^* \Delta t}.$$

We will employ the following notation:

- $\lfloor \tilde{l} \rfloor$ - the greatest integer less than or equal to \tilde{l}

- $\lceil \tilde{l} \rceil$ - the least integer that is greater than or equal to \tilde{l}
- $\{\tilde{l}\}$ - the fractional part of \tilde{l}
- $t^* := (1 - \{\tilde{l}\})\Delta t + t_1$.

First, in the interval $[t_1, t^*]$, set

$$\lambda_* := v^* \lfloor \tilde{l} \rfloor (t^* - t_1).$$

Then, for $m \in \mathbb{N}$, $m \leq \lfloor \tilde{l} \rfloor$, define

$$S_m(t) := \frac{\lambda_*(m-1)}{\lfloor \tilde{l} \rfloor} + v^*(t - t_1).$$

We perform a similar construction in $(t^*, t_2]$, namely set

$$\lambda^* := v^* \lceil \tilde{l} \rceil (t_2 - t^*),$$

and for $m \in \mathbb{N}$, $m \leq \lceil \tilde{l} \rceil$, define

$$S_m(t) := \frac{\lambda^*(m-1)}{\lceil \tilde{l} \rceil} + v^*(t - t_1).$$

Then, define

$$S(t) := \begin{cases} \bigcup_{\substack{m \in \mathbb{N} \\ m \leq \lfloor \tilde{l} \rfloor}} \{S_m(t)\} & \text{if } t \in [t_1, t^*] \\ \bigcup_{\substack{m \in \mathbb{N} \\ m \leq \lceil \tilde{l} \rceil}} \{S_m(t)\} & \text{if } t \in (t^*, t_2] \end{cases}$$

The function S then maps t to the set of points in \mathbb{R} where we want to take slices of the cube at time t . Note that

$$\bigcup_{t \in [t_1, t_2]} S(t) = [0, 2r],$$

and further that every $\xi \in [0, 2r]$ belongs to $S(t)$ for only one t (See Figure 2.6).

Now define, for $t \in [t_1, t_2]$,

$$F_\eta^{k,\ell}(t) := \tilde{F}(S(t))$$

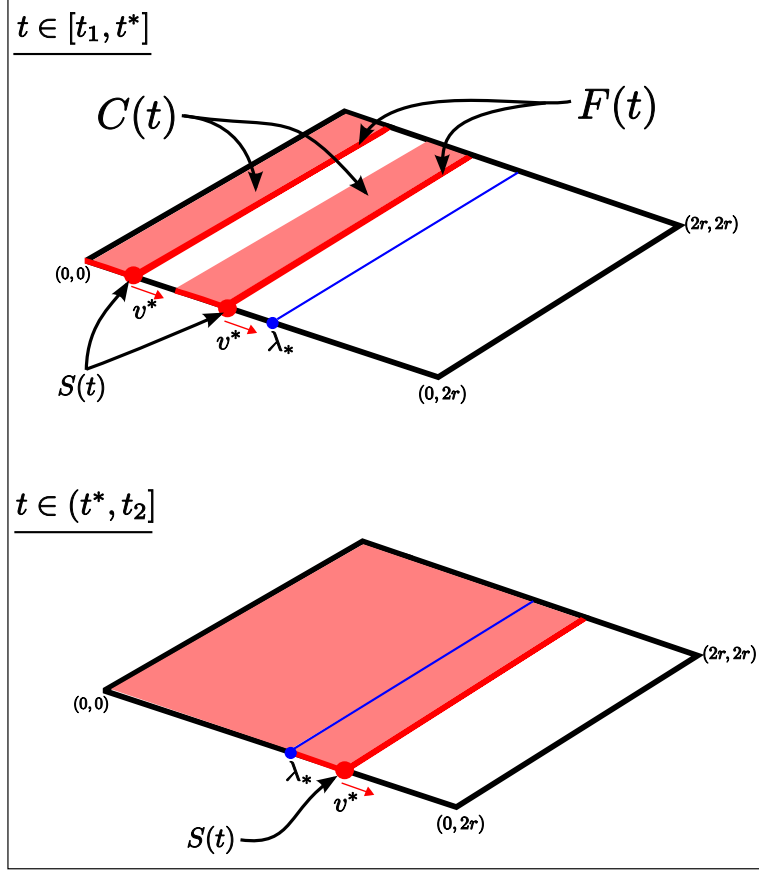


Figure 2.6: Slicing of a square with optimal front speed.

$$C_\eta^{k,\ell}(t) := \begin{cases} \bigcup_{\substack{m \in \mathbb{N} \\ m \leq \lfloor \tilde{l} \rfloor}} \{y \in G_\ell^k : S_m(t_1) \leq y^N \leq S_m(t)\} & \text{if } t \in [t_1, t^*] \\ \{y \in G_\ell^k : y^N \leq \lambda^*\} \cup \bigcup_{\substack{m \in \mathbb{N} \\ m \leq \lceil \tilde{l} \rceil}} \{y \in G_\ell^k : S_m(t^*) \leq y^N \leq S_m(t)\} & \text{if } t \in (t^*, t_2] \end{cases}$$

(see Figure 2.7). Note that by construction of the slices, $C_\eta^{k,\ell}(t) = G_\ell^k$. Then, in a manner similar to above, define the family of measures ρ_t^v , $t \in [t_1, t_2]$, by setting, for any Borel $A \subset Q_\ell^k$

$$\rho_t^v(A) := \int_{t_1}^{t_2} v^* \mathcal{H}^{N-2} (F_\eta^{k,\ell}(t) \cap A) dt.$$

For reasons similar to those used for the measures ρ_t , these measures are all well defined

Radon measures. Now, by applying the change of variables

$$\int_0^{\frac{(2r)}{\lambda}} \mathcal{H}^{N-2}(\tilde{F}(\lambda t))dt = \lambda \int_0^{2r} \mathcal{H}^{N-2}(\tilde{F}(t))dt,$$

to each of the slices individually, we find that

$$\rho_{t_2}^v(Q_\ell^k) = \rho_{2r}(Q_\ell^k), \quad (2.6.90)$$

however note that such an equality does not necessarily hold at any other time in $t \in [t_1, t_2]$. Also, with a similar restriction to one slice regions, the previous argument for the measures ρ_t can be modified to prove that $\forall t \in [t_1, t_2]$, we have that for any ball $B \subset Q_\ell^k$

$$(1 - \eta)|D\chi_{E_x}|(C_\eta^{k,\ell}(t) \cap B) \leq \rho_t^v(B) \leq |D\chi_{E_x}|(C_\eta^{k,\ell}(t) \cap B). \quad (2.6.91)$$

This means that $\forall t \in [t_1, t_2]$,

$$|D\chi_{E_x}|(C_\eta^{k,\ell}(t)) << \rho_t^v,$$

and that the densities

$$\gamma_t^v(x) := \frac{d(|D\chi_{E_x}|(C_\eta^{k,\ell}(t)))}{d\rho_t^v}(x)$$

exist $\forall t \in [t_1, t_2]$, ρ_t^v -a.e. $x \in Q_\ell^k$, and satisfy the uniform bounds

$$1 \leq \gamma_t^v \leq \frac{1}{1 - \eta}.$$

Therefore, for $\varphi \in C_0^1([t_1, t_2])$ and $f \in C_0(\Omega')$,

$$\int_{t_1}^{t_2} \dot{\varphi}(t) \int_{C_\eta^{k,\ell}(t) \cap Q(x,r)} f(x) d\mathcal{H}^{N-1}(x) dt = - \int_{t_1}^{t_2} \varphi(t) \int_{F_\eta^{k,\ell}(t)} f(x) v^* \gamma_t^v(x) d\mathcal{H}^{N-2}(x) dt.$$

Since for any $f \in C_0(\Omega')$, the map

$$t \mapsto \int_{C_\eta^{k,\ell}(t) \setminus Q_\ell^k} f(x) d\mathcal{H}^{N-1}(x)$$

is constant in $[t_1, t_2]$, we have

$$\int_{t_1}^{t_2} \dot{\varphi}(t) \int_{C_\eta^{k,\ell}(t) \setminus Q_\ell^k} f(x) d\mathcal{H}^{N-1}(x) dt = 0,$$

for any $\varphi \in C_0^1([t_1, t_2])$. Therefore we have that for $\varphi \in C_0^1([t_1, t_2])$ and $f \in C_0(\Omega')$

$$\int_{t_1}^{t_2} \dot{\varphi}(t) \int_{C_\eta^{k,\ell}(t)} f(x) d\mathcal{H}^{N-1}(x) dt = - \int_{t_1}^{t_2} \varphi(t) \int_{F_\eta^{k,\ell}(t)} f(x) v^* \gamma_t^v(x) d\mathcal{H}^{N-2}(x) dt.$$

Thus, in each time interval Y_ℓ^k the pair $(C_\eta^{k,\ell}, F_\eta^{k,\ell})$ satisfies the front representation, with front velocity $v_\eta^{k,\ell}(x, t) = \gamma_t^v(x)v^*$. Employing the uniform bounds on γ_t^v and (2.6.89) we have the following upper bound on the dissipation for the trajectory in the cube for η small enough:

$$\begin{aligned} \int_{t_1}^{t_2} \int_{F_\eta^{k,\ell}(t)} \psi(v_\eta^{k,\ell}(x, t)) d\mathcal{H}^{N-2}(x) dt &= \int_{t_1}^{t_2} \int_{F_\eta^{k,\ell}(t)} \psi(v^* \gamma_t(x)) d\mathcal{H}^{N-2}(x) dt \\ &\leq (1 + \delta)\mathcal{C} \int_{t_1}^{t_2} \int_{F_\eta^{k,\ell}(t)} v^* \gamma_t(x) d\mathcal{H}^{N-2}(x) dt \\ &= (1 + \delta)\mathcal{C} \int_{t_1}^{t_2} \int_{F_\eta^{k,\ell}(t)} v_\eta^{k,\ell}(x, t) d\mathcal{H}^{N-2}(x) dt. \end{aligned}$$

Part VI:

Repeat this construction in each cube Q_l^k during the time interval Y_l^k , and in this way define the functions C_η^k and F_η^k for \mathcal{L}^1 almost every $t \in I_k$. From Part V we have that the front representation formula holds in each time interval, which means that for $\varphi \in C_0^1(I_k)$ and $f \in C_0(\Omega')$

$$\begin{aligned} \int_{t_1}^{t_2} \dot{\varphi}(t) \int_{C_\eta^{k,\ell}(t)} f(x) d\mathcal{H}^{N-1}(x) dt &= - \int_{t_1}^{t_2} \varphi(t) \int_{F_\eta^{k,\ell}(t)} f(x) v^* \gamma_t^v(x) d\mathcal{H}^{N-2}(x) dt \\ &\quad + \int_{F_\eta^{k,\ell}(t_2)} f d\mathcal{H}^{N-2}(x) - \int_{F_\eta^{k,\ell}(t_1)} f d\mathcal{H}^{N-2}(x) \end{aligned}$$

where the boundary terms are the traces of the $L^1(I_k)$ function

$$t \mapsto \int_{F_\eta^{k,\ell}(t)} f d\mathcal{H}^{N-2}(x). \tag{2.6.92}$$

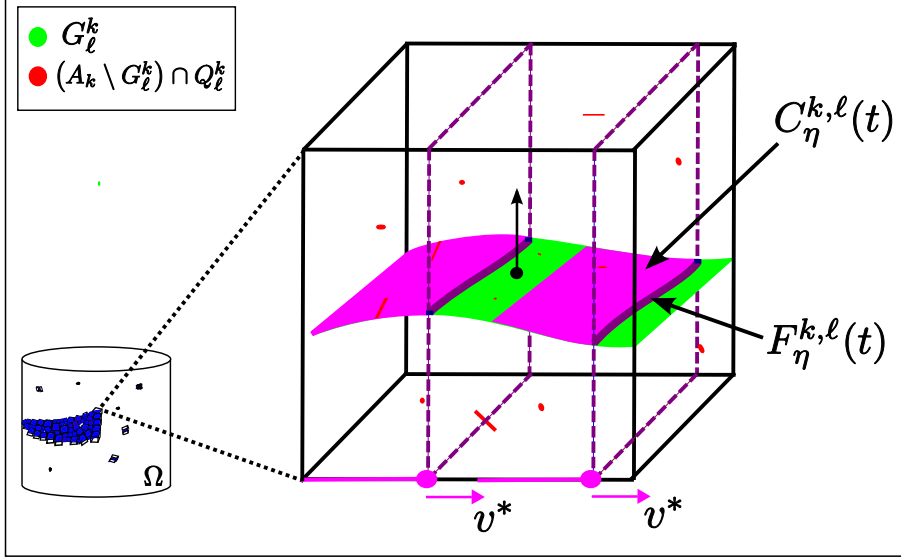


Figure 2.7: Defining the front in each cube through slicing.

Thus, by linearity of the integral we sum over all of the intervals Y_l^k , and use the fact that there are no jumps in the traces of the function (2.6.92) at the endpoints of each interval Y_l^k , to see that the front representation holds for C_η^k and F_η^k in I_k , i.e., for $\varphi \in C_0^1(I_k)$ and $f \in C_0(\Omega')$

$$\int_{t_1}^{t_2} \dot{\varphi}(t) \int_{C_\eta^k(t)} f(x) d\mathcal{H}^{N-1}(x) dt = - \int_{t_1}^{t_2} \varphi(t) \int_{F_\eta^k(t)} f(x) v_\eta^k d\mathcal{H}^{N-2}(x) dt.$$

Now, define A_{k+1} by setting

$$A_{k+1} := A_k \setminus C_\eta^k(I_k),$$

where by $C(I_k)$ we mean the C_η^k image of the set I_k . By the above we have

$$\begin{aligned} \mathcal{H}^{N-1}(A_{k+1}) &\leq \sum_{l=1}^{\infty} \frac{2}{k} \eta (2r_l^k)^{N-1} \\ &\leq \frac{2}{k} \frac{1}{1 - \frac{\eta}{k}} \mathcal{H}^{N-1}(A_k). \end{aligned} \tag{2.6.93}$$

Then, repeat the above construction for each A_k on the time interval I_k , $k > 1$, to define the functions C_η and F_η on all of $[a, b]$ (see Figure 2.8. We apply a similar argument to the above to show that the pair (C_η, F_η) satisfies the front representation formula

in $[0, T]$. Now, since $\{A_k\}_{k=1}^{\infty}$ is a decreasing sequence of \mathcal{H}^{N-1} measurable sets and $\mathcal{H}^{N-1}(A_k) < \infty$, by (2.6.93)

$$\mathcal{H}^{N-1}(C_{\eta}(b) \setminus \Gamma) = 0.$$

Since all of the time intervals are disjoint and cover almost all of $[a, b]$, we have that

$$\begin{aligned} \int_a^b \int_{F_{\eta}(t)} \psi(v(x, t)) d\mathcal{H}^{N-2}(x) dt &\leq (1 + \delta)\mathcal{C} \int_a^b \int_{F_{\eta}(t)} v_{\eta}(x, t) d\mathcal{H}^{N-2}(x) dt \\ &= (1 + \delta)\mathcal{C}\mathcal{H}^{N-1}(\Gamma). \end{aligned}$$

□

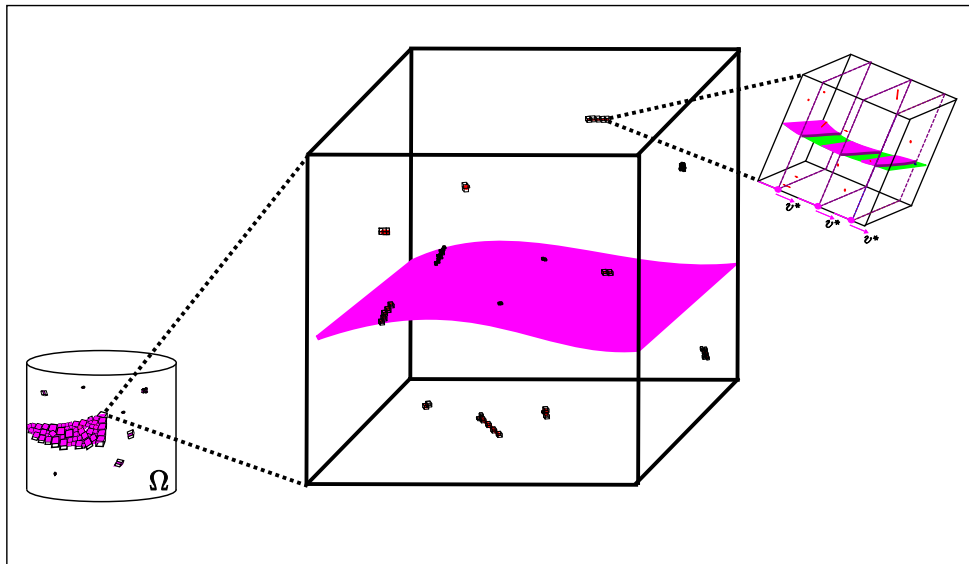


Figure 2.8: Inductive covering of the remaining pieces of Γ .

Now we prove the relaxation theorem.

Theorem 2.6.13. *Let $\psi : [0, \infty) \rightarrow [0, \infty)$ be continuous and*

$$I_{\epsilon}[q] := \int_0^T e^{-\frac{t}{\epsilon}} \int_{F(t)} \psi(v(x, t)) d\mathcal{H}^{N-2}(x) dt \quad (2.6.94)$$

for $q = (u, C) \in \mathcal{T}$. Then I_{ϵ}^* , the lower semicontinuous envelope in \mathcal{T}^* of the functional

I_ϵ , with respect to the convergence defined by (2.6.62), is given by

$$I_\epsilon^*[q] = \mathcal{C} \int_0^T e^{-\frac{t}{\epsilon}} d\mu(t), \quad (2.6.95)$$

where $q = (u, C) \in \mathcal{T}^*$, C^* is the minimal crack set trajectory associated to q , μ is the weak derivative of $t \mapsto \mathcal{H}^{N-1}(C^*(t))$, and

$$\mathcal{C} := \inf_{s \in (0, \infty)} \frac{\psi(s)}{s},$$

Proof. The proof proceeds as follows. First, we use the results of Theorem 2.6.12 to construct a sequence $\{q_i\}_{i=1}^\infty \subset \mathcal{T}$ such that $q_i \rightarrow q$ and whose energies converge to the right hand side of (2.6.95). Then we will combine this construction and the lower semicontinuity of the right hand side of (2.6.95) to complete the proof.

Let $q = (u, C) \in \mathcal{T}^*$ with associated C^* . We construct a sequence $\{q_j\}_{j=1}^\infty \subset \mathcal{T}$ that converges to q and achieves the lower bound in the limit through the following. Let \mathcal{D} be a countable dense subset of $[0, T]$ that generates q and contains the times 0 and T . For each $j \in \mathbb{N}$, choose

$$D_j := \{0 = t_0^j < t_1^j < \dots < t_j^j = T\} \subset \mathcal{D}$$

such that $\{D_j\}$ is an increasing sequence of nested sets and

$$\mathcal{D} = \bigcup_{j=1}^\infty D_j.$$

Now, fix $j \in \mathbb{N}$. By definition of \mathcal{T}^* , for each $t \in [0, T]$ $u(\cdot, t) \in SBV_p(\Omega')$ where $p > 1$. Also, since \mathcal{D} generates q then for every $t \in [0, T]$

$$C^*(t) \cong C_0 \cup \bigcup_{\substack{\tau \leq t \\ \tau \in \mathcal{D}}} S(u(\tau)).$$

Since $\mathcal{H}^{N-1}(C^*(t)) \leq \mathcal{H}^{N-1}(C^*(T)) < \infty$ for all $t \in [0, T]$, we can apply Lemma 2.6.10 and Theorem 2.6.12, so that for each interval $[t_k^j, t_{k+1}^j]$, $k = 0, \dots, j-1$, we can choose a

pair (C_k^j, F_k^j) satisfying the front representation and so that

$$C_k^j(t_{k+1}^j) \setminus C_k^j(t_k^j) \cong C^*(t_{k+1}^j) \setminus C^*(t_k^j) \quad (2.6.96)$$

and

$$\begin{aligned} \int_{t_k^j}^{t_{k+1}^j} \int_{F_k^j(t)} \psi(v_j(x, t)) d\mathcal{H}^{N-2}(x) dt &\leq \left(1 + \frac{1}{j}\right) \mathcal{H}^{N-1}(C^*(t_{k+1}^j) \setminus C^*(t_k^j)) \\ &= \left(1 + \frac{1}{j}\right) \int_{t_k^j}^{t_{k+1}^j} d|D\mathcal{H}^{N-1}(C^*(t))|. \end{aligned} \quad (2.6.97)$$

Repeat this process for each $k = 0, \dots, j-1$, and then define $\{q_j = (u_j, C_j)\}_{j=1}^\infty$ by setting

$$u_j(t) := \begin{cases} u(t_k^j) & \text{for } t \in [t_k^j, t_{k+1}^j) \\ u(T) & \text{for } t = T \end{cases}$$

and

$$C_j(t) := \begin{cases} C_k^j(t_k^j) & \text{for } t \in [t_k^j, t_{k+1}^j) \\ C^*(T) & \text{for } t = T. \end{cases}$$

Clearly we have for each $t \in \mathcal{D}$

$$u_j(\cdot, t) \rightarrow u(\cdot, t),$$

in fact for any such t there is an $M \in \mathbb{N}$ such that for all $j > M$, $u_j(\cdot, t) \equiv u(\cdot, t)$. Then, we have the upper bound

$$\begin{aligned} I_\epsilon[q_j] &= \sum_{k=0}^{j-1} \int_{t_k^j}^{t_{k+1}^j} e^{-\frac{t}{\epsilon}} \int_{F_j(t)} \psi(v_j(x, t)) d\mathcal{H}^{N-2}(x) dt \\ &\leq \left(1 + \frac{1}{j}\right) \mathcal{C} \sum_{k=0}^{j-1} \int_{t_k^j}^{t_{k+1}^j} e^{-\frac{t_k^j}{\epsilon}} d|D\mathcal{H}^{N-1}(C^*(t))|, \end{aligned}$$

and the lower bound

$$\begin{aligned} I_\epsilon[q_j] &= \sum_{k=0}^{j-1} \int_{t_k^j}^{t_{k+1}^j} e^{-\frac{t}{\epsilon}} \int_{F_j(t)} \psi(v_j(x, t)) d\mathcal{H}^{N-2}(x) dt \\ &\geq \mathcal{C} \sum_{k=0}^{j-1} \int_{t_k^j}^{t_{k+1}^j} e^{-\frac{t_k^j+1}{\epsilon}} d|D\mathcal{H}^{N-1}(C^*(t))|. \end{aligned}$$

Thus, we have

$$I_\epsilon[q_j] \rightarrow \mathcal{C} \int_0^T e^{-\frac{t}{\epsilon}} d|D\mathcal{H}^{N-1}(C^*(t))| \quad \text{as } j \rightarrow \infty. \quad (2.6.98)$$

We now combine the results above to complete the proof. For any $q = (u, C) \in \mathcal{T}^*$ with associated C^* , from Remark 2.6.11 and the sequence constructed in Part I, we have that

$$\mathcal{C} \int_0^T e^{-\frac{t}{\epsilon}} d\mu \geq I_\epsilon^*[q]. \quad (2.6.99)$$

The other inequality

$$I_\epsilon^*[q] \leq \mathcal{C} \int_0^T e^{-\frac{t}{\epsilon}} d\mu \leq I_\epsilon^*[q] \quad (2.6.100)$$

follows from the following. For any $\{q_i\}_{i=1}^\infty \subset \mathcal{T}$ such that $q_i \rightarrow q$. we again combine Remark 2.6.11 and Part I to construct a sequence \tilde{q}_i so that $\tilde{q}_i \rightarrow q$ with

$$\liminf_{i \rightarrow \infty} \mathcal{C} \int_0^T e^{-\frac{t}{\epsilon}} d\mu_i = \lim_{j \rightarrow \infty} I_\epsilon[\tilde{q}_j],$$

which combined with Lemma 2.6.9 gives (2.6.100). \square

Chapter 3

A Level Set Method for Mumford-Shah and Fracture

3.1 Introduction

The Mumford-Shah model for image segmentation ([23]) and variational models for fracture ([17]) are surprisingly similar: they both involve minimizing energies of the basic form

$$(u, \Gamma) \mapsto \int_{\Omega \setminus \Gamma} |\nabla u|^2 dx + \mathcal{H}^1(\Gamma),$$

where $\mathcal{H}^1(\Gamma)$ is the one-dimensional Hausdorff measure (i.e., length) of the set Γ , representing either the boundary of images (in the case of Mumford-Shah) or the fracture set. The domain $\Omega \subset \mathbb{R}^2$ represents either the image film or the reference configuration for the deformation u . Actually, the model for quasistatic fracture in [17] is the limit of a sequence of minimization problems of this form ([16]). For Mumford-Shah, there is the additional term

$$\int_{\Omega} |u - g|^2 dx,$$

where g is the initial image.

There has been much analysis of the properties of minimizers, mostly in the context of Mumford-Shah, and while the original Mumford-Shah conjecture – that there exists a minimizing pair in the class $u \in H^1(\Omega \setminus \Gamma)$, $\Gamma = \cup \Gamma_i$ where the union is finite and each Γ_i is a C^1 arc – remains open (since it is still unknown whether minimizers have Γ 's with only a finite number of connected components), the behavior of solutions is largely

understood (see [13] for a compilation of results). In particular, there is a characterization of all possible blow-up limits Γ of minimizing sets ([6]). The three possibilities are: i) Γ is a straight line (this corresponds to blowing up at a regular point of Γ), ii) Γ is a ray, such as a crack-tip in fracture (corresponding to blowing up at such a tip), iii) Γ is made of three rays, meeting at a triple junction with each angle equal to 120^0 .

This last property might seem odd, as it is the only junction allowed, and one might think that some minimizers would have quadruple junctions, such as in a checkerboard. However, it is not too hard to see that the total length of the boundary between the black and white squares on a checkerboard can be slightly reduced by replacing each quadruple junction with two nearby triple junctions (see figure 3.2.2 below), so that blow-up limits in this case are straight lines or triple junctions. We should also add that it is not known whether the type ii) “crack-tips” occur in Mumford-Shah minimizers, but this is certainly due to the fact that almost no explicit solutions are known, and the solutions that are known involve large degrees of symmetry in the domain and data. Solutions with these tips are generally believed to exist, and have been proven to exist for certain Dirichlet problems ([7]).

While Γ -convergence based numerical methods are theoretically justified (see, e.g., [5], [8]), there has naturally been interest in extending numerical methods for computing free boundaries to computing free discontinuities, particularly for the level set method of Osher and Sethian, [26]. Recently, Chan and Vese developed level set methods for computing the Mumford-Shah problem ([9],[28]) based on using two fields. Our interest in developing a new level set method for this problem is a result of these recent level set methods and their incompatibility with the second and third types of blow up limits, which we describe further below.

Now, we briefly outline the Vese-Chan algorithm. The starting point is the level set method for motion by mean curvature of Osher and Sethian, [26]. The idea is that, if one wants to evolve the boundary of a set A by its mean curvature, one can solve

$$\phi_t = \operatorname{div} \left(\frac{\nabla \phi}{|\nabla \phi|} \right),$$

$$\phi(0) = \text{signed distance from } \partial A.$$

Then, taking $A(t) := \{x : \phi(x, t) < 0\}$, it follows that $\partial A(t)$ moves by its mean curvature. The idea for extending this to variational problems is that, if there is a necessary condition for minimality involving the mean curvature of the boundary of a set A , then

an evolution law can be derived for a ϕ as above, so that the set $A(t)$ is stationary if and only if its boundary satisfies the necessary condition. Additionally, of course, one wants to design the evolution law so that if the set does not satisfy the condition, they move so that they are closer to satisfying it.

The Mumford-Shah functional is

$$\mathcal{E}(u, \Gamma) := \int_{\Omega \setminus \Gamma} (|u - g|^2 + |\nabla u|^2) dx + \mathcal{H}^1(\Gamma),$$

where g is a given L^∞ function [23]. Given $A(0)$ and the signed distance function ϕ , we consider the minimizer u of the above energy, with $\Gamma = \partial A(0)$. The corresponding energy can be written

$$\int_{\Omega \setminus \Gamma} E(x) dx + \mathcal{H}^1(\Gamma),$$

where $E(x) := |u(x) - g(x)|^2 + |\nabla u(x)|^2$. A necessary condition for minimality is that, for \mathcal{H}^1 almost every $x \in \Gamma$,

$$[E] = \kappa$$

for the correct orientation of the curvature κ (see [4]), where $[E]$ is the jump in E across Γ . The idea behind this can be seen by considering the case where E is larger on one side of Γ than the other, and Γ is flat. For definiteness, we can suppose that Γ is horizontal and E is larger above Γ than below. Then it would lower the total energy to perturb Γ upwards into the region of larger E , and extending the solution u from below into the the region that has been newly enclosed below Γ . The volume term would then be reduced by $[E]$ times the area of this region, and the surface term is increased by some amount. The equation $[E] = \kappa$ reflects these two effects canceling each other.

A straightforward adaptation of the level set method would then involve solving

$$\phi_t = [E] - \kappa = [E] - \operatorname{div} \left(\frac{\nabla \phi}{|\nabla \phi|} \right)$$

with appropriate initial conditions, but this would have the limitation that $\Gamma := \partial A(0)$ can divide Ω into only two regions: the set of points in A (i.e., where $\phi < 0$) and the set of points outside (i.e., where $\phi > 0$), so that, for example, triple junctions are impossible. Vese and Chan address this by using two level set functions, ϕ^1 and ϕ^2 , thereby gaining the ability to use four types of regions, or “colors”, to divide Ω : the set where both functions are negative, the set where just ϕ^1 is negative, etc. However, we

claim that this method retains some important deficiencies of the one-function level set method, and that the introduction of more functions does not satisfactorily overcome these deficiencies.

3.2 Revisiting the Vese-Chan algorithm

Here we identify three fundamental issues with the Vese-Chan algorithm (VCA), the first being a consequence of the inherent limitations of extending the usual level set methods to free discontinuity problems (in particular, discontinuity sets having crack-tips), the second is due to the independence of the zero level sets of the two fields in the algorithm (i.e., the fact that the two level sets do not interact with each other, for example, to combine into pairs of triple junctions when they cross, rather than forming a quadruple junction), and the third comes from the reliance on the Four Color Theorem (which would be a problem no matter how many level set functions are used).

3.2.1 Crack-tips

Since the curve Γ obtained by VCA is always a union of boundaries of sets, it is incapable of having a “crack tip” as illustrated in figure 3.1. Very few solutions of Mumford-Shah are known explicitly (and these tend to need very strong symmetry of the domain and data g), and in particular there is no known solution of Mumford-Shah that has a crack-tip. However, crack-tips are known to exist in global minimizers of Mumford-Shah (see [7]), which means, essentially, that we take $\Omega = \mathbb{R}^2$, the g term is removed, and u is said to be minimal if it has lower energy than any v satisfying $\{v \neq u\}$ compact support in \mathbb{R}^2 , where the energy comparison is on any open set S satisfying $\{v \neq u\}$ compact support in S . Furthermore, as mentioned above, these solutions are one of only three possible blow-up limits of solutions of Mumford-Shah. Finally, as the name “crack-tip” suggests, these solutions are of critical importance in variational models for crack growth. Indeed, Griffith’s criterion for crack growth [18], the basis for much recent work on variational methods for fracture mechanics, is a model for the growth of a crack from its tip.

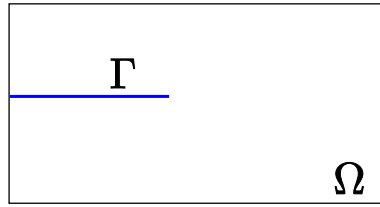


Figure 3.1: A Γ with a crack tip

3.2.2 Triple junctions

VCA penalizes the zero level sets of the fields ϕ_1, ϕ_2 in a similar way to how the Mumford-Shah energy penalizes the unknown set Γ . The problem is that the energy contribution of the zero level sets of the two fields should be the length of the union of these sets, rather than the sum of their lengths – the difference being that when the zero level sets overlap, there is a savings. For example, without this effect, changing a quadruple junction into two triple junctions increases the energy, and so VCA will not prefer these junctions.

The fact that the lengths are penalized separately can be seen from the fact that each level set function separately satisfies the necessary condition involving curvature, independent of the fact that they might overlap. Again, this may seem insignificant, as the odds might appear to be small that these sets would overlap. However, one effect of minimizing the Mumford-Shah energy (and a source of difficulty in analyzing solutions) is that discontinuity sets prefer to overlap, so that two nearby curves can be drawn to each other in order to overlap, thereby reducing the overall energy, since each curve is effectively penalized by only half its length in the overlap region. This is not taken into account in the existing level set methods.

The fact that methods such as VCA (as well as Ambrosio-Tortorelli [5]) will generally just find local minimizers, and this phenomenon of curves moving together in order to overlap might be a property of global minimizers but not local ones, might seem to rarely affect local minimization. However, it is critical at junctions, where curves can move arbitrarily small distances to form neighboring triple junctions and decrease the energy. One result of this is that the only possible junctions are still triple junctions, since, for example, it is not hard to see from Bonnet's characterization of global minimizers that a quadruple junction can split continuously (in L^2 and SBV , etc.) into two triple junctions while decreasing the total energy (see figure 3.2.2). Therefore, even

with local minimization, only triple junctions can occur. Yet, due to the independence of the level sets in VCA, there is no preference for these triple junctions, and any type of junction, e.g., quadruple, quintuple, can occur.

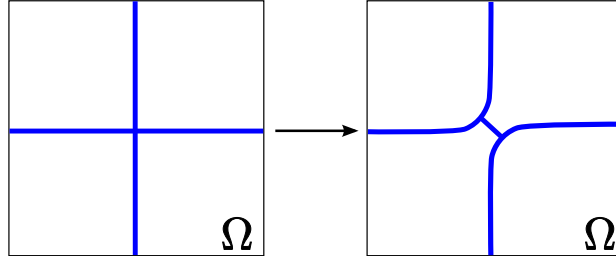


Figure 3.2: Energy of quadruple junction can be reduced by using two triple junctions

3.2.3 The Four Color Theorem

[28] relies on the Four Color Theorem in using two level set functions. The Four Color Theorem only means that a collection of objects *can* be colored using no more than four colors, and therefore two level set functions. But there must be deliberation in choosing how to color, as figure 3.3 shows: if all four colors are used in the outer four regions, there is no way to color the center region in a way that gives neighboring regions different colors. In VCA, if the initial seeding results in four “colors” for the outer objects, VCA will not detect the inner one.

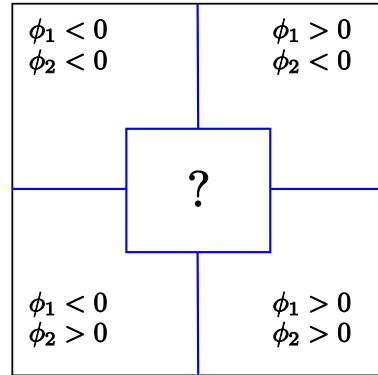


Figure 3.3:

3.3 Introduction to the proposed level set algorithm

In seeking to develop a level set method that does not suffer from the “crack-tip” limitation, among others, it seems necessary to replace the union of curves Γ by a thin neighborhood A of Γ , and evolve this region A by a level set method. The issue is, by what law should the boundary of A evolve? Our first focus will be on a part of A approximating a curve, as in figure 3.4. If we solve for the $u \in H^1(\Omega \setminus A)$ that minimizes

$$\int_{\Omega \setminus A} |u - g|^2 dx + \int_{\Omega \setminus A} |\nabla u|^2 dx, \quad (3.3.1)$$

and E is defined in the natural way so that, for the minimizer u , the above is equal to

$$\int_{\Omega \setminus A} E(x) dx,$$

then if the jump in energy from x^- “across A ” to x^+ , $[E] := E(x^+) - E(x^-)$, exceeds the outer curvature κ^+ (which, for now, we assume equals $-\kappa^-$ since A is thin), then ∂A should be perturbed upward, at both x^- and x^+ . A perturbation in the opposite direction would need to follow if, instead, the curvature exceeded the energy jump.

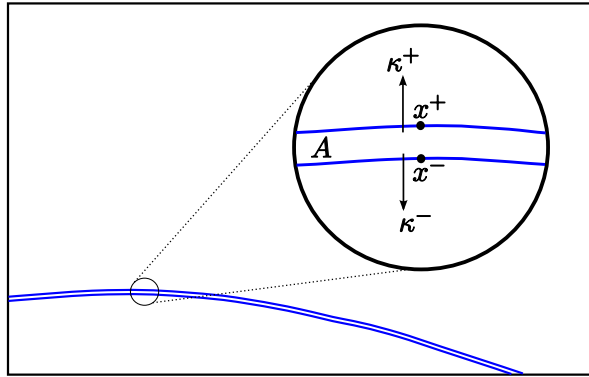


Figure 3.4:

Two problems now arise: how do we determine what point in ∂A is “across A ” from a particular $x^- \in \partial A$, and how do we communicate between these points to determine $[E]$? We do both implicitly as follows. Notice that (assuming we have satisfactorily

defined “across ”) the issue is only to find the sign of

$$[E] - \kappa. \quad (3.3.2)$$

If we consider the quantity $2E(x) - \kappa(x)$ at both x^- and x^+ , then an easy calculation shows that (3.3.2) equals half of

$$(2E(x^+) - \kappa^+) - (2E(x^-) - \kappa^-).$$

Therefore, the issue is simply to determine on which side of A the quantity $2E - \kappa$ is larger. Since A is presumed thin, a natural way to determine this, while implicitly defining “across”, is to solve

$$\Delta\psi = 0 \text{ in } A$$

$$\psi = 2E - \kappa \text{ on } \partial A.$$

Then, the normal derivative $\partial_\nu\psi$ at any x^- indicates whether $2E - \kappa$ is larger there, or on the other side of A . Taking $\phi(0)$ to be the signed distance function from ∂A , negative inside A , we then solve

$$\phi_t = \partial_\nu\psi$$

for a small time step, and the updated A is then the set on which $\phi(\Delta t) < 0$. We again minimize (3.3.1) with the new A , getting an updated u and E , and resolve for ψ , etc. Of course, several issues remain, such as how to keep A thin, and these will be discussed in later sections.

The case of a crack-tip in Γ is somewhat different. For an $x \in \partial A$ that is at a crack-tip, as in figure 3.5, there is no point of ∂A across from it, and so the situation is actually more straightforward and reminiscent of VCA. If A is perturbed outward at x , the region newly enclosed has zero energy, compared to $E(x)$ before the perturbation. So, if we were penalizing the length of ∂A , we would be interested in the sign of $E - \kappa$, as in VCA. However, we should not penalize the length of ∂A , but rather the length of the approximated Γ , or $1/2$ the length of ∂A . So, we are interested, again, in the sign of $2E - \kappa$. As E and κ will both be very large at a tip, and $2E - \kappa$ will be relatively quite small away from a tip, using $\partial_\nu\psi(x)$ to indicate the sign of $2E - \kappa$ at a crack-tip is a reasonable approximation.

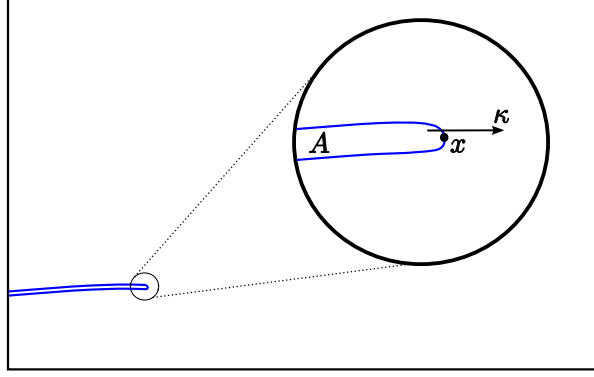


Figure 3.5:

3.4 The new level set method

In this section we present the details of our new level set method. First, in section 3.4.1, we give the formal description of the new level set method. Then, in section 3.4.2 we give the implementation details of the algorithm.

3.4.1 Formal Description

First, given an initial image g , we seed our algorithm as follows. We find $v \in H^1(\Omega)$ that minimizes

$$u \mapsto \int_{\Omega} |u - g|^2 dx + \int_{\Omega} |\nabla u|^2 dx. \quad (3.4.3)$$

We then set A_0 to be the set where $|\nabla v| \geq \gamma \|\nabla v\|_{\infty}$ for a chosen parameter $\gamma \in (0, 1)$ and we set $\phi(x, 0)$ to be the signed distance from ∂A_0 , negative in the interior of A_0 and positive outside. Then we find $u_1 \in H^1(\Omega \setminus A_0)$ that minimizes

$$u \mapsto \int_{\Omega \setminus A_0} |u - g|^2 dx + \int_{\Omega \setminus A_0} |\nabla u|^2 dx. \quad (3.4.4)$$

Then we set

$$E(x) := |u_0 - g|^2(x) + |\nabla u_0|^2(x) \quad (3.4.5)$$

and solve the PDE

$$\begin{cases} \Delta \psi = 0 & \text{in } A_0 \\ \psi = 2E - \kappa & \text{on } \partial A_0. \end{cases} \quad (3.4.6)$$

Here, κ is shorthand for the curvature of the level sets of ϕ ,

$$\kappa := \operatorname{div} \left(\frac{\nabla \phi}{|\nabla \phi|} \right). \quad (3.4.7)$$

Then, for any $x \in \partial A_0$, the sign of $\partial_\nu \psi$ indicates whether ψ is larger at x or at the point $x' \in \partial A_0$ “across” from x . For example, if

$$\partial_\nu \psi(x) > 0$$

then

$$\begin{aligned} 2E(x) - \kappa(x) &> 2E(x') - \kappa(x') \\ &= 2E(x') + \kappa(x), \end{aligned}$$

which reduces to

$$[E](x) := E(x) - E(x') > \kappa(x).$$

We then perturb A_0 appropriately. In the context of the above example, we would perturb A_0 outward at x and inward at x' . We do this by decreasing ϕ at x and increasing it at x' . Thus, we solve

$$\phi_t = -\partial_\nu \psi \text{ in } \partial A_0, \quad (3.4.8)$$

where we note that $\partial_\nu \phi(x') < 0$ if $\partial_\nu \psi(x) > 0$. This defines an approximation for $A(\Delta t)$ given by

$$A_1 := \{x : \phi(x, \Delta t) < 0\}.$$

We then redefine $\phi(x, \Delta t)$ to be the signed distance function from ∂A_1 and we repeat this process.

3.4.2 Computational details

In this section, we present the computational details of the algorithm described above. To obtain a finite element discretization, we choose a quasi-uniform and shape-regular triangulation $\mathcal{T}_h(\Omega)$ of Ω composed of triangular elements of size $O(h)$. All computations are performed on subdomains $\Omega' \subset \Omega$ such that no $\partial\Omega'$ cuts through any element of

$\mathcal{T}_h(\Omega)$, and we denote by $\mathcal{T}_h(\Omega')$ the triangulation $\mathcal{T}_h(\Omega)$ restricted to Ω' . All the relevant PDEs are solved by the finite element method using the space $V_h(\Omega') \subset H^1(\Omega')$ consisting of continuous piecewise linear functions on the triangulation $\mathcal{T}_h(\Omega')$.

Given a mesh $\mathcal{T}_h(\Omega')$, we will use the following notation for convenience:

$$\begin{aligned}\mathcal{N}(\Omega') &:= \{\text{set of all nodes } x_j \text{ in the mesh } \mathcal{T}_h(\Omega')\} \\ \mathcal{Z}_j(\Omega') &:= x_j \cup \{x_k \in \mathcal{N}(\Omega') : x_k \text{ connected to } x_j \text{ by an edge}\} \\ \mathcal{W}_j(\Omega') &:= \{\cup_k \tau_k \in \mathcal{T}_h(\Omega') : x_j \in \tau_k\}.\end{aligned}$$

We always assume that τ_k , \mathcal{W}_j , Ω' and Ω are closed regions, and $\mathcal{N}(\Omega')$ includes the nodes on $\partial\Omega'$. As part of our level set algorithm, we need to compute $\nabla v(x_j)$ (the gradient of a function at a node x_j of $\mathcal{N}(\Omega')$) for $v \in V_h(\Omega')$. Since ∇v is a piecewise constant function in Ω' , then we will need to “smooth” ∇u to give meaning to $\nabla v(x_j)$. The smoothing procedure is defined via Clement interpolation, that is, using the following average of ∇v over $\mathcal{W}_j(\Omega')$:

$$I_{\Omega'}^2(\nabla v)(x_j) = \frac{\sum_{\tau_k \in \mathcal{W}_j(\Omega')} \text{area}(\tau_k) \nabla v|_{\tau_k}}{\sum_{\tau_k \in \mathcal{W}_j(\Omega')} \text{area}(\tau_k)}.$$

Note that the smoothing procedure takes into account only elements τ_k in $\mathcal{T}_h(\Omega')$. We also need to compute the divergence of the relevant vector fields (in particular to compute curvatures). Thus, given a vector field p , we approximate $\nabla \cdot p$ at each $x_j \in \mathcal{N}(\Omega')$ as follows. First, we computing a linear function defined on $\mathcal{W}_j(\Omega')$ that is the least squares best fit of p_1 evaluated at the nodes of $\mathcal{Z}_j(\Omega')$. We repeat this for each component of p , and then sum the slopes of the linear approximations to calculate our approximation of $\nabla \cdot p$.

We also use Clement interpolation to smooth the relevant scalar fields on nodes of $\mathcal{N}(\Omega')$. Suppose w is a scalar field defined in $V_h(\Omega')$. Then:

$$I_{\Omega'}^1(w)(x_j) = \frac{\sum_{\tau_k \in \mathcal{W}_j(\Omega')} \text{area}(\tau_k) w|_{\tau_k}}{\sum_{\tau_k \in \mathcal{W}_j(\Omega')} \text{area}(\tau_k)}.$$

This smoothing procedure can be used to compute the divergence of a vector field defined on $(V_h(\Omega'))^2$.

We now describe the computational details of the algorithm for the first time iteration

($n = 0$). Recall that we are given an image function g defined on Ω . As described above, we begin by seeding the algorithm with a subdomain $A_0 \subset \Omega$. With this in mind, we minimize the problem (3.4.3) by the following finite element method: find $v \in V_h(\Omega)$ such that

$$\int_{\Omega} \nabla v \cdot \nabla \varphi \, dx + \int_{\Omega} v \varphi \, dx = \int_{\Omega} g \varphi \, dx \quad \forall \varphi \in V_h(\Omega).$$

We compute $I_{\Omega}^2 \nabla v \in V_h(\Omega)$ using the smoothing method described above, and then fix $\gamma \in (0, 1)$ to define the subregion $A_0 \subset \Omega$ by:

$$A_0 := \{x \in \Omega : |I_{\Omega}^2(\nabla v)(x)| \geq \gamma \max_{x_j \in \mathcal{N}(\Omega)} |I_{\Omega}^2(\nabla v)(x_j)|\}.$$

It is easy to see that A_0 is a polygonal domain with edges crossing elements of $\mathcal{T}_h(\Omega)$. Then we define the subdomain $A_0^h \subset A_0$ by:

$$A_0^h := \{\cup_k \tau_k \in \mathcal{T}_h(\Omega) : \text{all three vertices of } \tau_k \text{ belong to } A_0\},$$

i.e., A_0^h is the largest subdomain of A_0 composed by elements of $\mathcal{T}_h(\Omega)$. The definition of A_0^h and its complement $\Omega \setminus A_0^h$ lead to natural definitions of $\mathcal{T}_h(A_0^h)$, $\mathcal{N}(A_0^h)$, $V_h(A_0^h)$, $\mathcal{T}_h(\Omega \setminus A_0^h)$, $\mathcal{N}(\Omega \setminus A_0^h)$ and $V_h(\Omega \setminus A_0^h)$. These are the relevant sets for posing the finite element methods, while A_0 is relevant for defining the level set function ϕ_0 .

We define the level set function $\phi_0 \in V_h(\Omega)$ by computing the signed distance from each node of $\mathcal{N}(\Omega)$ to the boundary of A_0 . With the definition of A_0^h and ϕ_0 in hand, we solve the Dirichlet problem (3.4.6) by the following finite element method: find $\psi_0 \in V_h(A_0^h)$ such that $\psi_0(x_j) = 2E(x_j) - \kappa(x_j)$ for all nodes x_j on ∂A_0^h , and

$$\int_{A_0^h} \nabla \psi_0 \cdot \nabla \varphi \, dx = 0 \quad \forall \varphi \in V_h(A_0^h) \cap H_0^1(A_0^h). \quad (3.4.9)$$

To solve (3.4.9) we need to compute $E(x_j)$, defined by (3.4.5), and to compute the curvature $\kappa(x_j)$, defined by (3.4.7). To compute the energy $E(x_j)$ we first find $u_0 \in V_h(\Omega \setminus A_0^h)$ the solution of

$$\int_{\Omega \setminus A_0^h} \nabla u_0 \cdot \nabla \varphi \, dx + \int_{\Omega \setminus A_0^h} v \varphi \, dx = \int_{\Omega \setminus A_0^h} g \varphi \, dx \quad \forall \varphi \in V_h(\Omega \setminus A_0^h),$$

and then use the smoothing technique $I_{\Omega \setminus A_0^h}^2 \nabla u_0$ described above. Similarly, we compute the curvature $\kappa(x_j)$ by using the approximation to $\nabla \cdot \nabla \phi_0$ as described above.

We now evolve the level set function according to (3.4.8). This is done by finding $\hat{\phi}_1 \in V_h(\Omega)$ using a sort of Lax-Friedrichs discretization with a local timestepping δt_{x_j} :

$$\frac{\hat{\phi}_1(x_j) - I_h^1(\phi_0)(x_j)}{\delta t_{x_j}} = -\widetilde{\partial_\nu \psi_0}(x_j) \quad \forall x_j \in \Omega.$$

Here δt_{x_j} is chosen so that the zero level set curve does not move more than half of an element. The definition of the normal derivative $\widetilde{\partial_\nu \psi_0} \in V_h(\Omega)$ is done as follows: on nodes $x_j \in \mathcal{N}(A_0^h)$, we set $\widetilde{\partial_\nu \psi_0}(x_j)$ to be equal to $I_{A_0^h}^1(\nabla \psi_0 \cdot \nabla \phi_0)(x_j)$. On the remaining nodes $x_j \in \mathcal{N}(\Omega \setminus A_0^h) \setminus \mathcal{N}(A_0^h)$, we take the Dirichlet data $\widetilde{\partial_\nu \psi_0}$ on ∂A_0^h and perform the following discrete harmonic extension to $\Omega \setminus A_0^h$: find $\widetilde{\partial_\nu \psi_0} \in V_h(\Omega \setminus A_0^h)$ such that

$$\int_{\Omega \setminus A_0^h} \nabla \widetilde{\partial_\nu \psi_0} \cdot \nabla \varphi \, dx = 0 \quad (3.4.10)$$

for all $\varphi \in V_h(\Omega \setminus A_0^h)$ and vanishing on ∂A_0^h . The reason for using the discrete harmonic extension is because we want a smooth movement from ∂A_0 to ∂A_1 (the zero level set curve of $\hat{\phi}_1$) when outwards from A_0 . In order to decrease the complexity of the algorithm, we can replace this extension by a discrete harmonic extension to a thin layer of $\Omega \setminus A_0^h$ near ∂A_0^h , or to replace by some local averaging away from ∂A_0^h .

Now we repeat the process. We compute the signed distance function ϕ_1 associated to ∂A_1 , the compute A_1^h , u_1 , ψ_1 , $\widetilde{\partial_\nu \psi_1}$, $\hat{\phi}_2$, $\partial A_2, \phi_2$, A_2^h , u_2 etc. We point out that in regular level set methods, the level set functions $\hat{\phi}_n$ are the ones needed for computing rather than recomputing the signed distance functions ϕ_n . In our application, such a technique does not work properly because A_n is thin, and therefore, over many iterations the slope of $\hat{\phi}_n$ might get small and new zero level sets might appear, instead of zero level sets only existing due to the evolution of the original zero level sets.

We now describe two departures from the description in 3.4.1 which seem to be necessary computationally. First, instead of simply solving (3.4.6) we actually solve the Poisson problem $\Delta \psi = -2$, i.e., we replace (3.4.9) with

$$\int_{A_0^h} \nabla \psi_0 \cdot \nabla \varphi \, dx = 2 \int_{A_0^h} \varphi \, dx \quad \forall \varphi \in V_h(A_0^h) \cap H_0^1(A_0^h). \quad (3.4.11)$$

This is an ad hoc technique we use to keep our domain thin. However, using this did result in our domain becoming too thin. Thus, we use another routine that enforces

a minimum thickness of the domain A_n . The idea of our technique is provided in the following pseudocode:

```

for each node  $x_j$  with small  $I_h^2(\nabla\phi_n)(x_j)$ 
    if  $\text{dist}(x_j, \partial A_n) < (\text{minimum domain thickness})$ 
        set  $\frac{\hat{\phi}_{n+1}(x_j) - I_h^1(\phi_n)(x_j)}{\delta t_{x_j}} = -1$ 
    end

```

3.5 Numerical results

We have tested our algorithm using the Mumford-Shah functional on a number of image functions, including those with overlapping objects. Also, we have verified that, when used with the energy used to model fracture, the algorithm is able to resolve crack tips.

Triple Junctions

To show that our method does find triple junctions, we used an image function $g : [0, 2] \times [0, 2] \rightarrow \mathbb{R}$ given by

$$g(x_1, x_2) := \begin{cases} 0 & \text{for } x_1 \leq 1 \text{ and } x_2 \leq 1 \\ 10 & \text{for } x_1 > 1 \text{ and } x_2 \leq 1 \\ 20 & \text{for } x_1 > 1 \text{ and } x_2 > 1 \\ 30 & \text{for } x_1 \leq 1 \text{ and } x_2 > 1. \end{cases}$$

The corresponding image for g is pictured below in Figure 3.6.

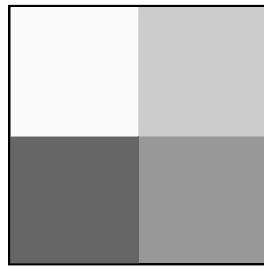


Figure 3.6: Initial image function to show triple junction

As discussed above, the minimizer of the Mumford-Shah functional for this image

function does not have a quadruple junction, since the energy can be reduced by using two triple junctions:

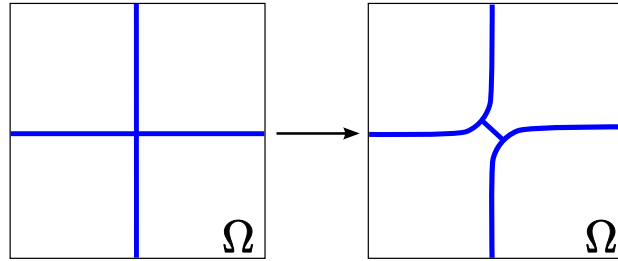


Figure 3.7: Recall: Energy of quadruple junction can be reduced by using two triple junctions

Figure 3.8 shows the results of our algorithm for the image function g defined above and using our seeding algorithm described in Section 3.4. Figure 3.9 is a zoom in of the final result that more clearly shows the triple junction. These computations were performed on a mesh generated by Triangle [27] composed of 77,574 triangles. We note that the number of iterations needed to compute the solution can be reduced by seeding our algorithm with an A_0 that approximates the quadruple junction created by the four color regions.

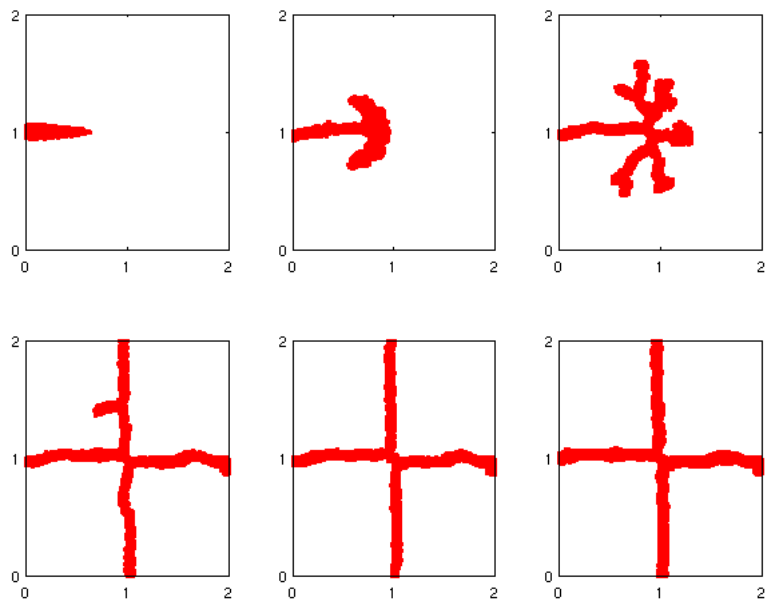


Figure 3.8: Results of our algorithm with image g

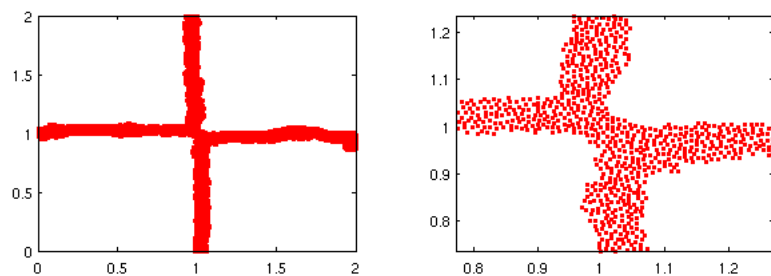


Figure 3.9: Results with a zoom in on junction at right

Table of Notation

$B(x, r)$	Closed ball centered at x with radius r	9
$E \subset\subset F$	\bar{E} compact and $\bar{E} \subset F$	1
$Q(x, r)$	Cube centered at x with side length $2r$	9
$\text{dist}(x, A)$	inf of $ x - y $ over $y \in A$	1
W	Elastic energy density	9
\mathcal{H}^n	n -dimensional Hausdorff measure	8
$K_i \xrightarrow{H} K$	$\{K_i\}$ converges to K in the Hausdorff metric	9
$A \cong B$	$\mathcal{H}^{N-1}(A \setminus B) = 0$	9
\bar{A}	Topological closure of A	1
$A \tilde{\subset} B$	$\mathcal{H}^{N-1}(A \setminus B) = 0$	9
\mathcal{L}^n	n -dimensional Lebesgue measure	8
2^X	Power set of X	9
$u_n \xrightarrow{SBV} u$	$\{u_n\}$ SBV-converges to u	9
$SBV_p(\Omega)$	$u \in SBV(\Omega)$ with $\nabla u \in L^p(\Omega)$	8
ν_E	Measure theoretic outer normal to E	9
$\partial^* E$	Reduced boundary of E	9
$SBV(\Omega)$	Special Functions of Bounded Variation on Ω	8
$S(u)$	Approximate discontinuity set of $u \in BV$	8
E_ξ^w	ξ super level set of $w \in BV$	9
$[u](x)$	Jump of u at x	27
C^*	Minimal crack trajectory for $(u, C) \in \mathcal{T}^*$	21
\mathcal{D} generates q		22
$\phi_t(A)$	Imbedding of $A \subset \mathbb{R}^{N-1}$ into \mathbb{R}^N by $x_N = t$	33
\mathcal{T}	Class of front representable trajectories	19

$\mathcal{T}_{p'}$	Class of constrained front representable trajectories	10
\mathcal{T}^*	Class of general trajectories	19
ψ	Dissipation potential	45
$\bar{\psi}$	Rate-independent envelope of ψ	19
\mathcal{C}	Slope of the rate-independent envelope of ψ	19
$\sigma(t, A)$	$N - 1$ -dimensional slice of the set A at $x_N = t$	33
$\mathcal{T}_h(\Omega)$	Shape-regular triangulation of Ω	58
$I_{\Omega'}^1(w)(x_j)$	Clement interpolation of scalar function w at node x_j	59
$I_{\Omega'}^2(p)(x_j)$	Clement interpolation of vector field p at node x_j	58
$\mathcal{N}(\Omega')$	set of all nodes x_j in the mesh $\mathcal{T}_h(\Omega')$	58
$\mathcal{Z}_j(\Omega')$	The set formed by the node x_j and all nodes connected to it by an edge	58
$\mathcal{W}_j(\Omega')$	The set of triangles that neighbor node x_j	58

Bibliography

- [1] J. Alberty, C. Carstensen, and S. A. Funken. Remarks around 50 lines of Matlab: short finite element implementation. *Numer. Algorithms*, 20(2-3):117–137, 1999.
- [2] L. Ambrosio. A compactness theorem for a new class of functions of bounded variation. *Boll. Un. Mat. Ital. B* (7), 3(4):857–881, 1989.
- [3] L. Ambrosio and A. Braides. Energies in SBV and variational models in fracture mechanics. In *Homogenization and applications to material sciences (Nice, 1995)*, volume 9 of *GAKUTO Internat. Ser. Math. Sci. Appl.*, pages 1–22. Gakkōtoshō, Tokyo, 1995.
- [4] L. Ambrosio, N. Fusco, and D. Pallara. *Functions of bounded variation and free discontinuity problems*. Oxford Mathematical Monographs. The Clarendon Press Oxford University Press, New York, 2000.
- [5] L. Ambrosio and V. M. Tortorelli. On the approximation of free discontinuity problems. *Boll. Un. Mat. Ital. B* (7), 6(1):105–123, 1992.
- [6] A. Bonnet. On the regularity of edges in image segmentation. *Ann. Inst. H. Poincaré Anal. Non Linéaire*, 13(4):485–528, 1996.
- [7] A. Bonnet and G. David. Cracktip is a global Mumford-Shah minimizer. *Astérisque*, (274):vi+259, 2001.
- [8] B. Bourdin and A. Chambolle. Implementation of an adaptive finite-element approximation of the Mumford-Shah functional. *Numer. Math.*, 85(4):609–646, 2000.
- [9] T. F. Chan and L. A. Vese. Active contours without edges. *IEEE Transactions on Image Processing*, 10(2):266–277, 2001.

- [10] B. D. Coleman and W. Noll. The thermodynamics of elastic materials with heat conduction and viscosity. *Archive for Rational Mechanics and Analysis*, 13:167–179, 1963.
- [11] G. Dal Maso and R. Toader. A model for the quasi-static growth of brittle fractures: existence and approximation results. *Arch. Ration. Mech. Anal.*, 162(2):101–135, 2002.
- [12] Gianni Dal Maso, Gilles A. Francfort, and Rodica Toader. Quasistatic crack growth in nonlinear elasticity. *Arch. Ration. Mech. Anal.*, 176(2):165–225, 2005.
- [13] G. David. *Singular sets of minimizers for the Mumford-Shah functional*, volume 233 of *Progress in Mathematics*. Birkhäuser Verlag, Basel, 2005.
- [14] E. De Giorgi and L. Ambrosio. New functionals in calculus of variations. In *Nonsmooth optimization and related topics (Erice, 1988)*, volume 43 of *Ettore Majorana Internat. Sci. Ser. Phys. Sci.*, pages 49–59. Plenum, New York, 1989.
- [15] L. C. Evans and R. F. Gariepy. *Measure theory and fine properties of functions*. Studies in Advanced Mathematics. CRC Press, Boca Raton, FL, 1992.
- [16] G. A. Francfort and C. J. Larsen. Existence and convergence for quasi-static evolution in brittle fracture. *Comm. Pure Appl. Math.*, 56(10):1465–1500, 2003.
- [17] G. A. Francfort and J.-J. Marigo. Revisiting brittle fracture as an energy minimization problem. *J. Mech. Phys. Solids*, 46(8):1319–1342, 1998.
- [18] A. Griffith. The phenomenon of rupture and flow in solids. *Phil. Trans. Roy. Soc. London*, 221-A:163–198, 1920.
- [19] C. J. Larsen, M. Ortiz, and C. L. Richardson. Fracture paths from front kinetics: Relaxation and rate-independence. *Arch. Ration. Mech. Anal.* To Appear.
- [20] C. J. Larsen, C. L. Richardson, and M. Sarkis. A level set method for the Mumford-Shah functional and fracture. *SIAM J. Imag. Sci.* Submitted.
- [21] A. Mielke. Evolution in rate-independent systems (ch. 6). In C.M. Dafermos and E. Feireisl, editors, *Handbook of Differential Equations, Evolutionary Equations, vol. 2*, pages 461–559. Elsevier B.V., 2005.

- [22] A. Mielke and M. Ortiz. A class of minimum principles for characterizing the trajectories of dissipative systems. *ESAIM Control Optim. Calc. Var.*, 2007. in press.
- [23] D. Mumford and J. Shah. Optimal approximations by piecewise smooth functions and associated variational problems. *Comm. Pure Appl. Math.*, 42(5):577–685, 1989.
- [24] P. Paris and F. Erdogan. A critical analysis of crack propagation laws. *Transactions of the ASME*, 85:528–534, 1963.
- [25] A. J. Rosakis, J. Duffy, and L. B. Freund. The determination of dynamic fracture toughness of aisi 4340 steel by the shadow spot method. *Journal of the Mechanics and Physics of Solids*, 32(4):443–460, 1984.
- [26] J. Sethian and S. J. Osher. The design of algorithms for hypersurfaces moving with curvature-dependent speed. In *Nonlinear hyperbolic equations—theory, computation methods, and applications (Aachen, 1988)*, volume 24 of *Notes Numer. Fluid Mech.*, pages 544–551. Vieweg, Braunschweig, 1989.
- [27] J. R. Shewchuk. Triangle: Engineering a 2D Quality Mesh Generator and Delaunay Triangulator. In Ming C. Lin and Dinesh Manocha, editors, *Applied Computational Geometry: Towards Geometric Engineering*, volume 1148 of *Lecture Notes in Computer Science*, pages 203–222. Springer-Verlag, May 1996. From the First ACM Workshop on Applied Computational Geometry.
- [28] L. A. Vese and T. F. Chan. A multiphase level set framework for image segmentation using the Mumford and Shah model. *International Journal of Computer Vision*, 50(3):271–293, 2002.
- [29] E. H. Yoffe. The moving griffith crack. *Philosophical Magazine*, 42:739–750, 1951.
- [30] W. P. Ziemer. *Weakly differentiable functions*, volume 120 of *Graduate Texts in Mathematics*. Springer-Verlag, New York, 1989. Sobolev spaces and functions of bounded variation.